

Searching for the signatures of terrestrial planets in F-, G-type main-sequence stars [★]

J. I. González Hernández^{1,2}, E. Delgado-Mena³, S. G. Sousa³, G. Israelian^{1,2}, N. C. Santos^{3,4}, V. Zh. Adibekyan³, and S. Udry⁵

¹ Instituto de Astrofísica de Canarias (IAC), E-38205 La Laguna, Tenerife, Spain
e-mail: jonay@iac.es

² Depto. Astrofísica, Universidad de La Laguna (ULL), E-38206 La Laguna, Tenerife, Spain

³ Centro de Astrofísica, Universidade do Porto, Rua das Estrelas, 4150-762 Porto, Portugal

⁴ Departamento de Física e Astronomia, Faculdade de Ciências, Universidade do Porto, Portugal

⁵ Observatoire Astronomique de l'Université de Genève, 51 Ch. des Maillettes, -Sauverny- Ch1290, Versoix, Switzerland

Received July 24, 2012; accepted ...

ABSTRACT

Context. Detailed chemical abundances of volatile and refractory elements have been discussed in the context of terrestrial-planet formation during the last years.

Aims. The HARPS-GTO high-precision planet-search program has provided an extensive database of stellar spectra which we have inspected in order to select the best-quality spectra available of late type stars. We have studied the volatile-to-refractory abundance ratios to investigate their possible relation with the low-mass planetary formation.

Methods. We present a fully differential chemical abundance analysis using high-quality HARPS and UVES spectra of 61 late F- and early G-type main-sequence stars, 29 are planet hosts and 32 are stars without detected planets.

Results. As the previous sample of solar analogs, these stars slightly hotter than the Sun also provide very accurate Galactic chemical abundance trends in the metallicity range $-0.3 < [\text{Fe}/\text{H}] < 0.4$. Stars with and without planets show similar mean abundance ratios. Moreover, when removing the Galactic chemical evolution effects, these mean abundance ratios, $\Delta[\text{X}/\text{Fe}]_{\text{SUN-STARS}}$, versus condensation temperature tend to exhibit less steep trends with nearly null or slightly negative slopes. We have also analyzed a sub-sample of 26 metal-rich stars, 13 with and 13 without known planets, with spectra at $S/N \sim 850$ on average, in the narrow metallicity range $0.04 < [\text{Fe}/\text{H}] < 0.19$ and find the similar, although not equal, abundance pattern with negative slopes for both samples of stars with and without planets. Using stars at $S/N \geq 550$ provides equally steep abundance trends with negative slopes for both stars with and without planets. We revisit the sample of solar analogs to study the abundance patterns of these stars, in particular, 8 stars hosting super-Earth-like planets. Among these stars having very low-mass planets, only four of them reveal clear increasing abundance trends versus condensation temperature.

Conclusions. Finally, we have compared these observed slopes with those predicted using a simple model which enables us to compute the mass of rocks which have formed terrestrial planets in each planetary system. We do not find any evidence supporting the conclusion that the volatile-to-refractory abundance ratio is related to the presence of rocky planets.

Key words. stars: abundances — stars: fundamental parameters — planetary systems — stars: atmospheres

In the last decade the exhaustive search for extra-solar planets has given rise to a significant collection of high-quality spectroscopic data (see e.g. Marcy et al. 2005; Udry & Santos 2007). In particular, the HARPS-GTO high-precision planet-search program (Mayor et al. 2003) has conducted in the first five years an intensive tracking of F-, G-, and K-type main-sequence stars in the solar neighborhood, resulting in the discovery of an increasing population of Neptune and super-Earth-like planets (Mayor & Udry 2008; Mayor et al. 2011). Interestingly, the very strong correlation observed between the host star metal-

licity (Santos et al. 2001, 2004; Valenti & Fischer 2005) and the occurrence frequency of giant planets appears to almost vanish when dealing with these less massive planets (Udry et al. 2006; Sousa et al. 2008, 2011; Mayor et al. 2011; Adibekyan et al. 2012c; Buchhave et al. 2012). In addition, most of Neptune and super-Earth-like planets are found in multi-planetary systems (see e.g. Mayor et al. 2009). Mayor et al. (2011) has recently announced the discovery of 41 planets with HARPS, among which there are 16 super-Earth-like planets. Many of these planets belong to complex planetary systems with a variety of planet masses and orbital properties (see e.g. Lovis et al. 2011), thus challenging our understanding of planet formation and evolution.

The search for peculiarities in the chemical abundance patterns of planet-host stars has been also performed (see e.g. Gilli et al. 2006; Ecuivillon et al. 2006; Neves et al. 2009; Adibekyan et al. 2012b), suggesting only small differences in some element abundance ratios between “single” stars (hereafter, “single” refers to stars without detected planets) and planet

[★] Based on observations collected with the HARPS spectrograph at the 3.6-m telescope (072.C-0488(E)), installed in the La Silla Observatory, ESO (Chile), with the UVES spectrograph at the 8-m Very Large Telescope (VLT) (program IDs: 67.C-0206(A), 074.C-0134(A), 075.D-0453(A)), installed in the Cerro Paranal Observatory, ESO (Chile), and with the UES spectrograph at the 4.2-m William Herschel Telescope (WHT), installed in the Spanish Observatorio del Roque de los Muchachos of the Instituto de Astrofísica de Canarias, in the island of La Palma

hosts (see the introduction in González Hernández et al. 2010, for a more detailed background). However, Adibekyan et al. (2012b,a), based on HARPS and Kepler data, have found that planet-host stars show significant enhancement of alpha elements at metallicities slightly below solar and belong to the Galactic thick disk. They found that at metallicities $[\text{Fe}/\text{H}] < -0.3$ dex, 13 planet hosts (HARPS and Kepler samples) out of 17 (about 76 %) are enhanced in alpha elements while only 32 % of stars without known planets are alpha-enhanced at a given metallicity. Thus, planet formation requires certain amount of metals and therefore, at relatively low metallicity, $[\text{Fe}/\text{H}] < -0.3$ dex, planet-host stars tend to be alpha-enhanced and tend to belong to the chemically defined thick disk where the stars should have higher overall metallicity Adibekyan et al. (2012a). This result may be supported by theoretical studies based on core-accretion models (see e.g. Mordasini et al. 2012).

Recently, Meléndez et al. (2009) has found an anomalous but small (~ 0.1 dex) volatile-to-refractory abundance ratio of a sample of 11 solar twins when compared to the solar ratio. They interpreted this particularity as a signature of the presence of terrestrial planets in the solar planetary system. In this study they used high-S/N and high-resolution spectroscopic data. Later on, this conclusion was also supported by Ramírez et al. (2009) who analyzed a sample of 64 solar analogs, but their result was not so evident, at least, not at the level of the accuracy of the abundance pattern shown in Meléndez et al. (2009) where the element abundances are at a distance of ≤ 0.015 dex from the mean abundance pattern (see also Ramírez et al. 2010; Schuler et al. 2011a). González Hernández et al. (2010) analyzed a sample of 7 solar twins, 5 without and 2 with planets, using very high-quality HARPS spectroscopic data, but maybe still small to confirm the result by Meléndez et al. (2009). However, González Hernández et al. (2010) found that on average both stars with and without detected planets seem to exhibit very similar abundance pattern, even when considering a metal-rich sub-sample of 14 planet hosts and 14 solar analogs. It is important to note that González Hernández et al. (2010) analyzed stars with planets of different minimum masses from Jupiter-mass to super-Earth planets. Nevertheless, the sample in Ramírez et al. (2009) contains same planet-host stars but these authors did not distinguish and/or mention them which may lead to confusing results. The results found by Meléndez et al. (2009) have not been fully confirmed (see also Ramírez et al. 2010; González Hernández et al. 2011a; Gonzalez et al. 2010; Gonzalez 2011; Schuler et al. 2011b), in particular the relation with presence of planets is strongly debated (González Hernández et al. 2010, 2011b). Recently, they however have found a similar abundance pattern in the solar twin HIP 56948 which they claim may have terrestrial planets (Meléndez et al. 2012).

Delgado Mena et al. (2010) have shown that the chemical abundance pattern of the planet-host stars can be used to distinguish among the different composition of the possible terrestrial planets. In fact, theoretical simulations based on the observed variations in the chemical abundances of host stars predict diverse compositions for extrasolar terrestrial planets, indeed quite different from those of the solar planetary system (Carter-Bond et al. 2012a).

In this paper, we investigate in detail the chemical abundances of “hot” analogs (hereafter, “hot” analogs refers to late F- and early G-type main-sequence stars hotter than the Sun, at temperatures $T_{\text{eff}} \sim 6175$ K) of the HARPS GTO sample, which have narrower convective zones than Sun-like stars, with the aim of searching for enhanced signature of terrestrial planets in their

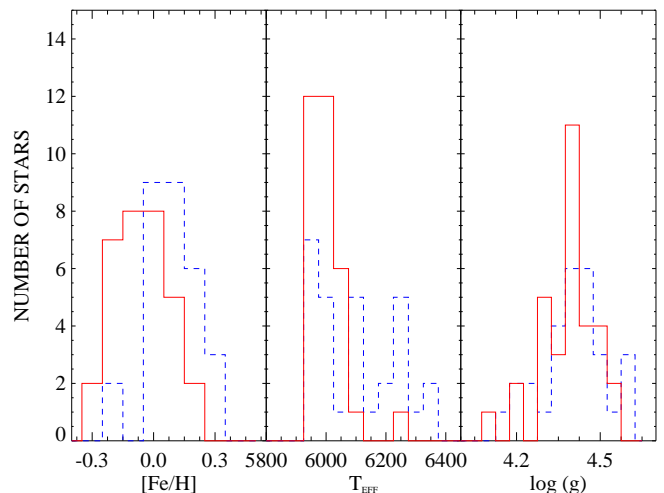


Fig. 1. Histograms of the stellar parameters and metallicities of the whole sample of “hot” analogs hosting planets (blue dashed lines) and without known planets (red solid lines).

Table 2. Ranges of stellar parameters and metallicities in different samples

Sample ^a	T_{eff}	$\log g$	$[\text{Fe}/\text{H}]$	N_{stars}^b
	[K]	[dex]	[dex]	
HA	5950–6400	4.14–4.60	-0.30 – +0.35	61
mrHA	5950–6400	4.14–4.60	+0.04 – +0.19	26

Notes. ^(a) Stellar samples: “hot” analogs, “HA”, metal-rich “hot” analogs, “mrHA”. ^(b) Total number of stars including those with and without known planets.

abundance patterns. We also re-analyze the data of solar analogs presented in González Hernández et al. (2010) taking into account the new discovered planets (see e.g. Mayor et al. 2011). We pay special attention to eight solar analogs harbouring super-Earth-like planets under the assumption that these small planets may have similar chemical composition to that of terrestrial or Earth-like planets.

1. Observations

In this study, as in González Hernández et al. (2010), we analyze high-resolution and high-S/N spectroscopic data obtained with three different telescopes and instruments: the 3.6m-ESO/HARPS at the *Observatorio de La Silla* in Chile, the 8.2m-VLT/UVES at the *Observatorio Cerro Paranal* in Chile and the 4.2m-WHT/UES at the *Observatorio del Roque de los Muchachos* in La Palma, Spain. In Table 1, we provide the wavelength ranges, resolving power, S/N and other details of these spectroscopic data.

The data were reduced in a standard manner, and latter normalized within the package IRAF¹, using low-order polynomial fits to the observed continuum.

¹ IRAF is distributed by the National Optical Observatory, which is operated by the Association of Universities for Research in Astronomy, Inc., under contract with the National Science Foundation.

Table 1. Spectroscopic observations

Spectrograph	Telescope	Spectral range	$\lambda/\delta\lambda$	Binning	N_{stars}^a	S/N ^b	δ S/N ^c	$\Delta\text{S/N}^d$
		[Å]		[Å/pixel]				
HARPS	3.6m-ESO	3800–6900	110,000	0.010	50	877	429	265–2015
UVES	8m-VLT	4800–6800	85,000	0.016	7	722	150	510–940
UES	4.2m-WHT	4150–7950	65,000	0.029	4	643	180	520–850

Notes. Details of the spectroscopic data used in this work. The UVES and UES stars are all planet-hosts. Three of the UVES stars were observed with a slit of 0.3'' providing a resolving power $\lambda/\delta\lambda \sim 110,000$. ^(a) Total number of stars including those with and without known planets. ^(b) Mean signal-to-noise ratio, at $\lambda = 6070$ Å, of the spectroscopic data used in this work. ^(c) Standard deviation from the mean signal-to-noise ratio. ^(d) Signal-to-noise range of the spectroscopic data.

Table 3. Stellar parameters and metallicities from the UVES and UES spectra

HD	T_{eff}	δT_{eff}	$\log g$	$\delta \log g$	ξ_t	$\delta \xi_t$	[Fe/H]	$\delta[\text{Fe}/\text{H}]$
	[K]	[K]	[dex]	[dex]	[km s ⁻¹]	[km s ⁻¹]	[dex]	[dex]
209458 ^a	6118	22	4.50	0.04	1.21	0.03	0.03	0.02
2039 ^a	5959	31	4.45	0.04	1.26	0.03	0.32	0.02
213240	6022	19	4.27	0.05	1.25	0.02	0.14	0.01
23596 ^b	6134	35	4.25	0.08	1.30	0.04	0.31	0.03
33636	5994	17	4.71	0.02	1.79	0.02	-0.08	0.01
50554 ^b	6129	50	4.41	0.07	1.11	0.06	0.01	0.04
52265 ^a	6136	46	4.36	0.04	1.32	0.06	0.21	0.03
72659	5951	13	4.30	0.02	1.42	0.01	0.03	0.01
74156	6099	19	4.34	0.03	1.38	0.02	0.16	0.01
89744 ^b	6349	43	3.98	0.05	1.62	0.05	0.22	0.03
9826 ^b	6292	43	4.26	0.06	1.69	0.05	0.13	0.03

Notes. Stellar parameters, T_{eff} and $\log(g/\text{cm s}^2)$, microturbulent velocities, ξ_t , and metallicities, [Fe/H], and their uncertainties, of the planet-host stars observed with UVES/VLT and UES/WHT spectrographs.

^(a) Stars observed with the UVES spectrograph at VLT telescope at $\lambda/\delta\lambda \sim 110,000$. The other stars were observed with UVES at $\lambda/\delta\lambda \sim 85,000$.

^(b) Stars observed with the UES spectrograph at WHT telescope at $\lambda/\delta\lambda \sim 65,000$.

2. Sample

With the aim of performing a detailed chemical analysis, we select late F- and early G-type stars with spectra at $\text{S/N} > 250$ from these three spectrographs. We end up with a sample of 29 planet-host stars and 32 “single” stars (see Fig. 1). All UVES and UES stars are planet hosts. In Table 2 we provide the ranges of stellar parameters and metallicities of the 61 “hot” analogs of the sample. In Fig. 1, we display the histograms of the effective temperatures, surface gravities and metallicities of this sample. The stars hosting planets are on average more metal-rich than the stars without known planets. Thus, we define a sub-sample of metal-rich of late F- and early G-type stars with $0.04 < [\text{Fe}/\text{H}] < 0.19$, containing 13 planet hosts and 13 “single” stars (see Table 2). On the other hand, due to the new planets recently discovered (see e.g. Mayor et al. 2011), in the sample of solar analogs presented in González Hernández et al. (2010), there are now 33 stars with planets and 62 stars without planets.

3. Stellar Parameters

The stellar parameters and metallicities of the HARPS stars were extracted from the work by Sousa et al. (2008), which are based on the equivalent widths (EWs) of 263 Fe I and 36 Fe II lines,

measured with the code ARES² (Sousa et al. 2007) and evaluating the excitation and ionization equilibria. For the UVES and UES stars we decided to re-computed the stellar parameters (see Table 3) using these higher quality data. Chemical abundances of Fe lines were derived using the 2002 version of the LTE code MOOG (Sneden 1973), and a grid of Kurucz ATLAS9 plane-parallel model atmospheres (Kurucz 1993).

4. Chemical abundances

We perform a fully differential analysis, at least, internally consistent. Thus, we have used the HARPS solar spectrum³ of the *Ganymede*, a *Jupiter*’s satellite, as solar reference (see González Hernández et al. 2010). We note here that the UVES and UES stars were also analysed using the HARPS *Ganymede* spectrum as solar reference due to the lack of an appropriate solar spectrum observed with these two instruments.

We compute the EW of each spectral line using the code ARES (Sousa et al. 2007) for most of the elements. However, as in González Hernández et al. (2010), for O, S and Eu, we cal-

² The ARES code can be downloaded at <http://www.astro.up.pt/>

³ The HARPS solar spectrum can be downloaded at <http://www.eso.org/sci/facilities/lasilla/instruments/harps/inst/monitoring/sun.html>

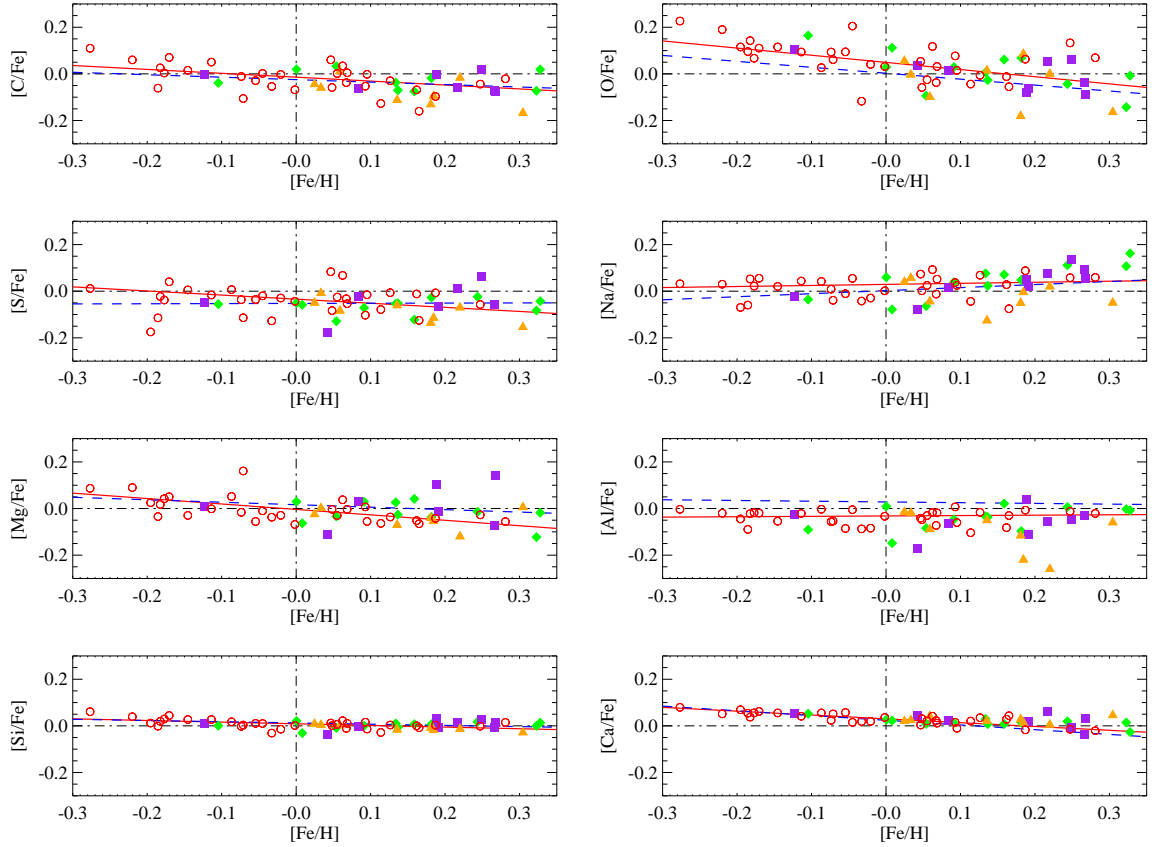


Fig. 2. Chemical abundance ratios $[X/Fe]$ versus $[Fe/H]$ for the whole sample of “hot” analogs, containing 32 “single” stars (red open circles) and 29 stars hosting planets, with the most massive planet in an orbital period $P_{\text{orb}} < 65$ days (green filled diamonds), $115 < P_{\text{orb}} < 630$ days (violet filled squares), $950 < P_{\text{orb}} < 4050$ days (orange filled triangles). Red solid lines provide linear fits to the data points of the 32 “single” stars, whereas blue dashed lines show the linear fits to the data points of “single” solar analogs in González Hernández et al. (2010).

culate the EW by integrating the line flux; and for Zr, by performing a gaussian fit taking into account possible blends. In both cases, we use the task `splor` within the IRAF package. The EWs of Sr, Ba and Zn lines were checked within IRAF, because, as well as for the elements O, S, Eu and Zr, for some stars, ARES did not find a good fit due to numerical problems and/or bad continuum location. For further details see Sect. 5 in González Hernández et al. (2010).

The oxygen abundance was derived from the forbidden $[O\text{I}]$ line. This line is severely blended with a NiI line (see e.g. Allende Prieto et al. 2001). We adopted the atomic parameters for Ni line from Allende Prieto et al. (2001) while for $[O\text{I}]$ line from Lambert (1978). For more details see Ecuivillon et al. (2006). We derive the EW of Ni line using the mean Ni abundance of the star and we subtract this EW from the global EW of the $[O\text{I}]$ feature. The remaining EW give us the O abundance of the star. In the solar case, the atlas solar spectrum (Kurucz et al. 1984), the whole feature has an EW of ~ 5.4 mÅ which provides an abundance⁴ of $A(\text{O}) = 8.74$ dex (see González Hernández et al. 2010, for more details).

We again use MOOG (Snedden 1973) and ATLAS models (Kurucz 1993) to derive the abundance of each line and thus, we determine the mean abundance of each element relative to its solar abundance in a line-by-line basis. However, to avoid problems with wrong EW measurements of some spectral lines,

we rejected all the lines with an abundance different from the mean abundance by more than a factor of 1.5 times the rms. We also checked that we get the same results when using a factor of 2 times the rms, but we decided to stay in a more restrictive position. The line-by-line scatter in the differential abundances goes on average, for 34 F- and G-type stars without planets in our sample, the line-by-line scatter goes on average from $\sigma \sim 0.014 - 0.025$ for elements like Si, Ni, Cr, Ca and Ti, to $\sigma \sim 0.035$ for C and Sc, to $\sigma \sim 0.050$ for Mg and Na and to $\sigma \sim 0.063$ for S. These numbers are comparable to those found in solar analogs (see González Hernández et al. 2010).

5. Discussion

In this section we will inspect the abundance ratios of different elements as a function of the metallicity, $[Fe/H]$, as well as the relation, for different samples of “hot” analogs, between the abundance difference, $\Delta[X/Fe]_{\text{SUN-STARs}}$, and the 50% equilibrium condensation temperature, T_C (see Lodders 2003). We will also explore the abundance pattern of some particular stars containing super-Earth-like planets in the sample of both “hot” analogs and solar analogs.

5.1. Galactic abundance trends

In Figs. 2, 3 and 4 we depict the very accurate abundance ratios $[X/Fe]$ of many elements in this sample of late F- and

⁴ $A(X) = \log[N(X)/N(H)] + 12$

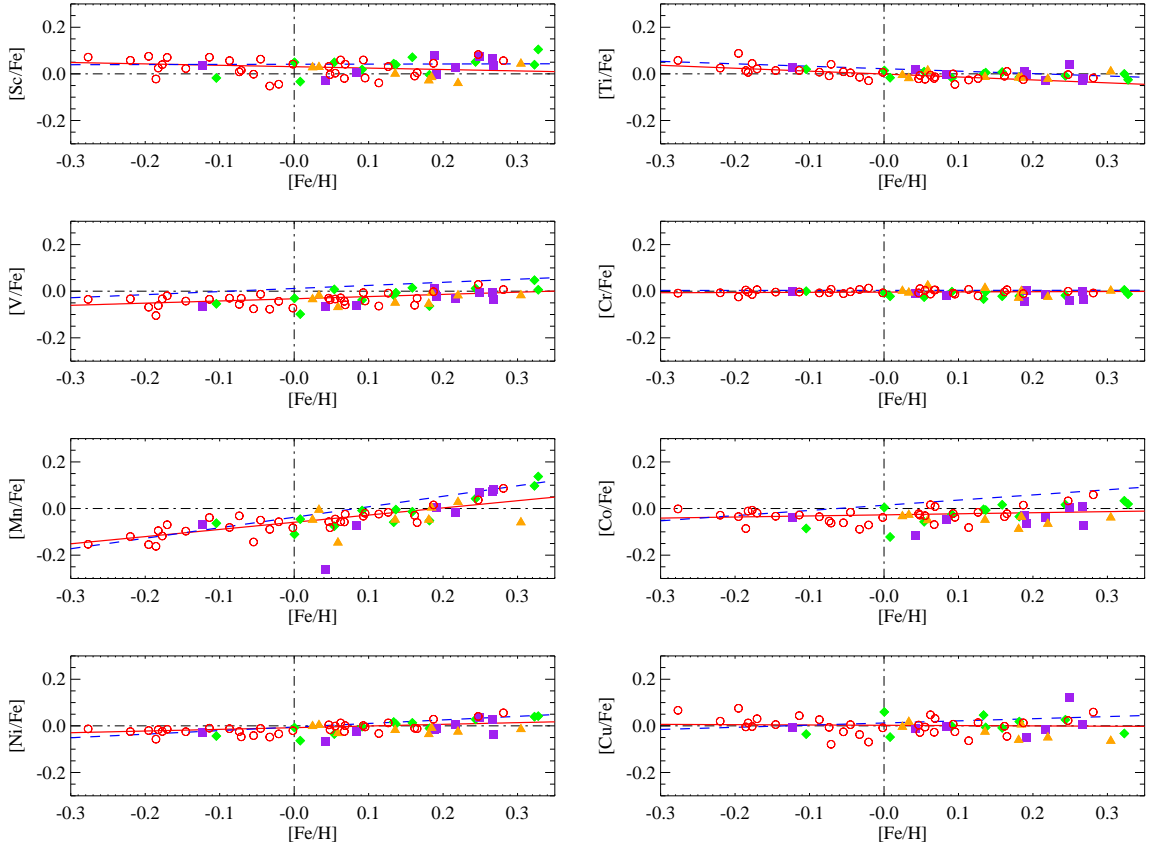


Fig. 3. Same as Fig. 2 but for other elements.

early G-type stars with and without planets, derived from the high-quality HARPS, UVES and UES spectra. These Galactic trends are compatible with those of Galactic thin disk stars (see e.g. Bensby et al. 2005; Reddy et al. 2006; Gilli et al. 2006; Takeda 2007; Neves et al. 2009; Delgado Mena et al. 2010; Adibekyan et al. 2012c) and, in particular, with those of solar analogs (Ramírez et al. 2009; González Hernández et al. 2010). We may note the small differences in the fits to the abundances of the “single” “hot” analogs and “single” solar analogs. In particular, the element O reveals slight differences at the lowest metallicities (i.e. at $[\text{Fe}/\text{H}] \sim -0.3$ in this sample) whereas Mn, Co, Sr, Ba, Ce and Nd present these small differences at the highest metallicities (i.e. at $[\text{Fe}/\text{H}] \sim +0.3$ in this sample). There is also a tiny shift of $\sim 0.03 - 0.05$ in the fits of Al and V. However, in general for the rest of the elements like S, Si, Ca, Ti, Cr and Ni, we almost find a perfect agreement. In Tables A.1–A.8 we provide the element abundance ratios $[X/\text{Fe}]$ which are all available online⁵.

5.2. Mean abundance ratios $[X/\text{Fe}]$ versus T_C : previous results

Meléndez et al. (2009) suggested that the formation of rocky planets in the solar system affect the composition of solar photosphere, by lowering the amount of refractory elements with respect to the volatile elements. They focus on Earth-like planets and do not comment on how much the formation of other

slightly more massive planets like super-Earth and Neptune like planets would affect their interpretation of the mean abundance pattern of solar twins with respect to the Sun.

According to the element abundances of the Earth (Kargel & Lewis 1993), the bulk composition of a terrestrial planet should be dominated by O, Fe, Mg and Si, with small amounts of Ca and Al, and very little C. These terrestrial planets would be composed by Mg silicates and metallic Fe with other species present in relatively minor amounts. Water and other hydrous may or may not be present (Bond et al. 2010). The composition of Earth-like planets depends on the chemical composition of host star (Bond et al. 2010; Carter-Bond et al. 2012a; Delgado Mena et al. 2010), and a wide variety of terrestrial planets compositions is predicted. Also giant planet migration plays an important role in the final Earth-like compositions (Carter-Bond et al. 2012b). A variation of $\pm 25\%$ from the Earth composition should be considered to include Venus and Mars as terrestrial planets (Carter-Bond et al. 2012a).

Depending of the final compositions these Earth-like planets could have substantial amount of water and develop plate tectonics (Carter-Bond et al. 2012b), which have been proposed as necessary condition for life. Simulations of super-Earth-like planets reveal that these slightly more massive planets could also have plate tectonics (Valencia et al. 2007a). These authors consider unlikely, although possible, that super-Earth-like planets could have a lot of gas (Valencia et al. 2007b), they state that at larger masses than $10 M_{\oplus}$, there exist a possibility that H and He is retained although these could give rise to massive ocean planets with high H_2O content and a relatively small layer of gas above it (Valencia et al. 2007b). We should note however that these simulations of super-Earth-like planets assumed a given

⁵ The online Tables A.1–A.8 are available in electronic form at the CDS via anonymous ftp to cdsarc.u-strasbg.fr (130.79.128.5) or via <http://cdsarc.u-strasbg.fr/viz-bin/qcat?J/A+A/...>

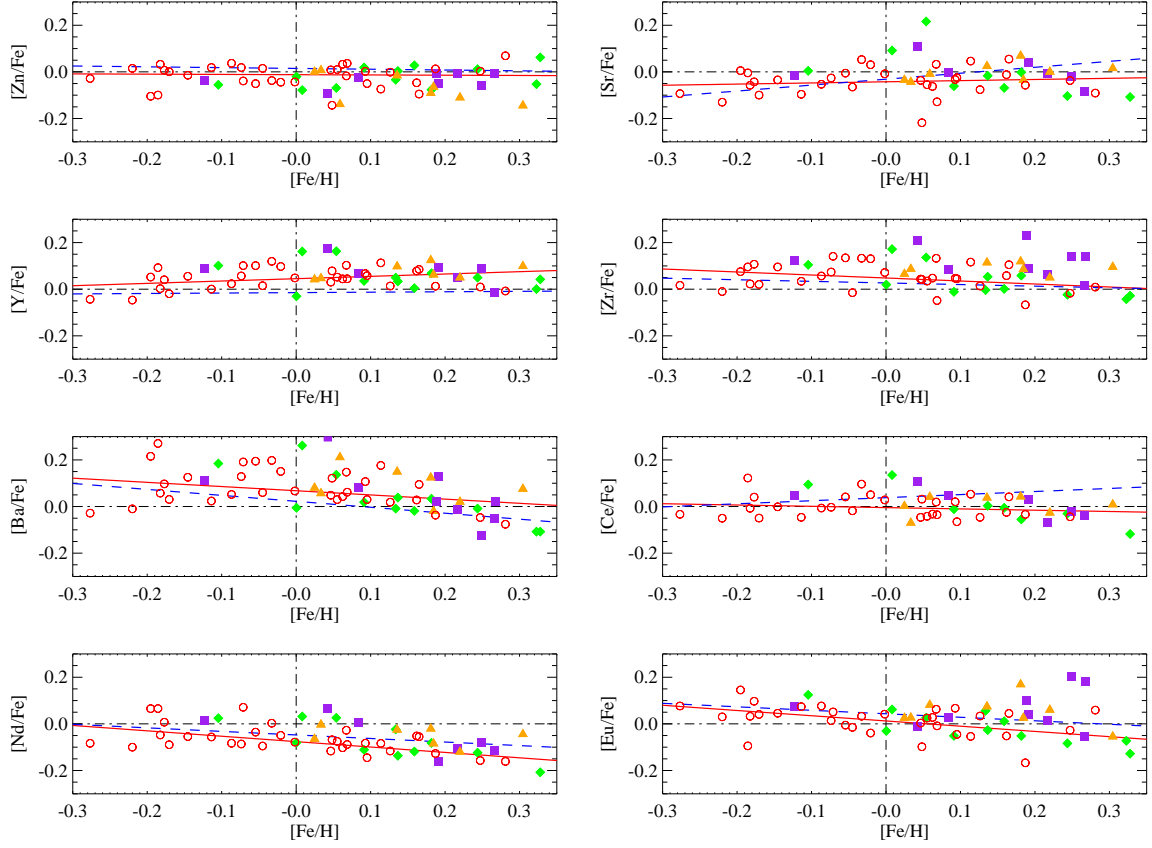


Fig. 4. Same as Fig. 2 but for other elements.

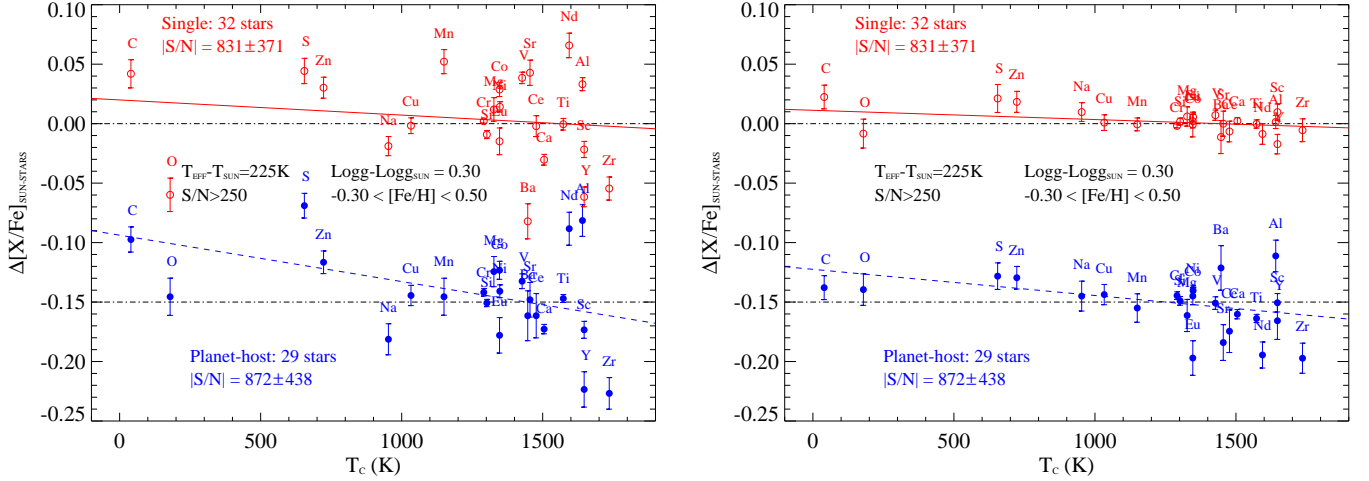


Fig. 5. Mean abundance differences, $\Delta[X/Fe]_{\text{SUN-STARS}}$, between the Sun, and 29 planet hosts (blue filled circles) and 32 “single” stars (red open circles) of the sample of all “hot” analogs. Error bars are the standard deviation from the mean divided by the square root of the number of stars. The points of stars hosting planets have been artificially shifted by -0.15 dex for the sake of clarity. Linear fits to the data points weighted with the error bars are also displayed for planet hosts (dashed line) and “single” stars (red solid line). The right panel shows the results after removing the galactic chemical evolution effects using the linear fits to the 32 “single” stars.

planetary composition similar to Earth-like planets, but it seems reasonable to assume that super-Earth-like planets, being formed in the same protoplanetary disk, could become a larger counterpart of Earth-like planets and therefore have similar composition.

Ramírez et al. (2009) derived the slopes of trends described by the abundance ratios of a sample of solar analogs versus the condensation temperature, T_c . Although they only took into account those elements with $T_c > 900$ K, they argued that, following the reasoning in Meléndez et al. (2009), a negative slope is an indication that a star should not have terrestrial planets even

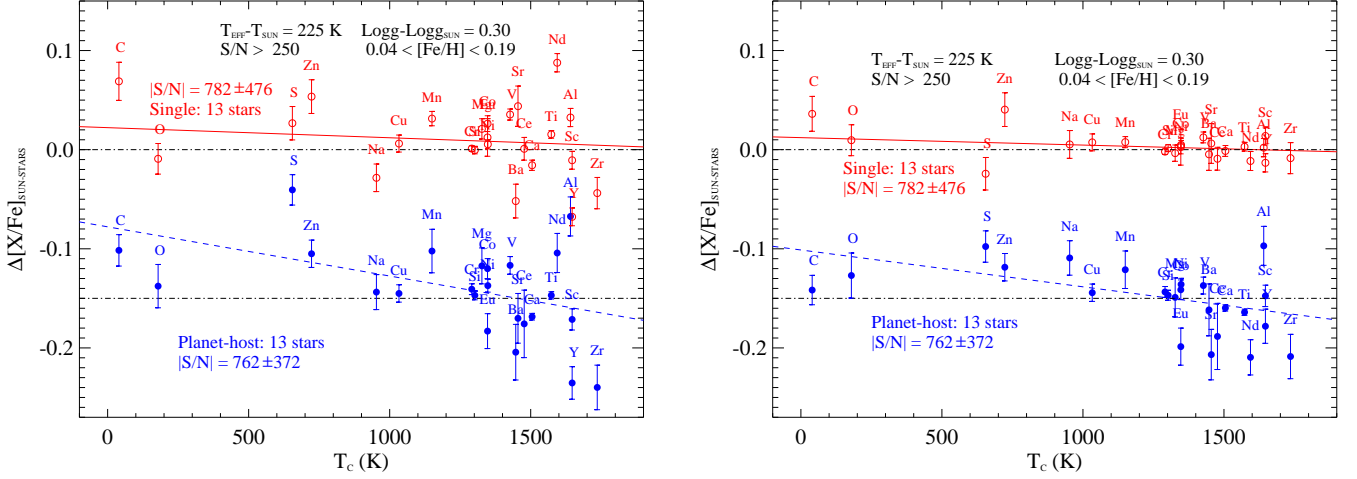


Fig. 6. Same as in Fig. 5 for 13 planet hosts and 13 “single” stars of the sample of metal-rich “hot” analogs.

if this star already contains giant planets. We note in this paper, as in González Hernández et al. (2010), we are evaluating the abundance differences $\Delta[X/Fe]_{\text{SUN-STARS}}$, and thus we follow the same reasoning as in Meléndez et al. (2009). Meléndez et al. (2009) also analyzed 10 solar analogs, among which four have close-in giant planets. Their abundance pattern differ from that of the Sun but resembles that of their solar twins. Although the result was statistically not significant, they suggest that stars with and without close-in giant planets should reveal different abundance patterns.

González Hernández et al. (2010) studied the abundance trends of solar analogs with and without planets and they found that most of these stars have negative slopes, and hence indicating that these stars should not contain terrestrial planets. Two stars in the sample by González Hernández et al. (2010), HD 1461 and HD 160691, with super-Earth-like planets provide abundance trends $[X/Fe]_{\text{SUN-STARS}}$ versus condensation temperature, T_c , with the opposite slope to that expected if these stars would contain terrestrial planets. Therefore, González Hernández et al. (2010) suggested that these abundance patterns are not related to the presence of terrestrial planets. They also noted that the abundance patterns of solar analogs are strongly affected by chemical evolution effects, especially for elements with steep Galactic trends like Mn (with $T_c \sim 1160$ K).

Ramírez et al. (2010) combined chemical abundance data of solar analogs from previous studies. They produced an average abundance pattern consistent with their expectations (Ramírez et al. 2009) but extracted from more noisy abundance patterns. They also argued that when deriving the slopes for elements with $T_c > 900$ K in the two planet hosts HD 1461 and HD 160691, they obtained the sign consistent with the results by Ramírez et al. (2009). González Hernández et al. (2011b) demonstrated instead that using the elements $T_c > 1200$ K provide the opposite sign as the case of $T_c > 900$ K. Unfortunately there are more refractory elements, most of them with $T_c > 1200$ K than volatile elements. Thus a more reliable trend should consider the whole range of T_c values for the available elements, i.e. $0 < T_c < 1800$ K (González Hernández et al. 2011b). In addition, subtracting the Galactic chemical evolution effects before fitting the abundance ratio $[X/Fe]$ almost completely removes any trend not from these two planet-host stars but also from the average values of the sub-sample of metal-rich solar analogs González Hernández et al. (2011a).

Gonzalez et al. (2010); Gonzalez (2011) investigated the abundances of refractory and volatile elements in a smaller sample of stars with and without giant planets. They claimed to confirm the results by Ramírez et al. (2009) but in a broader effective temperature, T_{eff} , range. They also stated that more metal-rich stars display steeper trends than more metal-poor counterparts. Schuler et al. (2011b) analyzed a small sample of 10 stars known to host giant planets using very high-S/N and very high-resolution spectra but in the wide T_{eff} range 5600–6200 K and in the metallicity, $[Fe/H]$, range 0–0.4 dex. They chose instead to fit the abundances $[X/H]$ versus T_c and found positive slopes in four stars with close-in giant planets and flat or negative slopes in stars with planets at longer orbital periods, thus consistent with recent suggestions of the terrestrial planet formation signature. They evinced however that these trends probably result of Galactic chemical evolution effects.

More recently, Schuler et al. (2011a) and Ramírez et al. (2011) have presented a detailed chemical analysis of the two solar twins of the 16 Cygni binary system. One of them, 16 Cygni B contains a Jupiter-mass planet orbiting in an eccentric orbit, but no planet has been detected around 16 Cygni A. According to Schuler et al. (2011a), these two stars appear to be chemically identical, with a mean difference of 0.003 ± 0.015 dex. On the other hand, Ramírez et al. (2011) found that star A is more metal-rich than star B by 0.041 ± 0.007 dex, and suggested that this may be related to the formation of giant planet in star B. Both results may be consistent at the $3-\sigma$ level and probably indicate that internal systematics are larger than typically assumed. Takeda (2005) claimed there is no metallicity difference between 16 Cygni A and B. Laws & Gonzalez (2001) were the first in performing a differential analysis and they also suggested that star A is more metal-rich than star B by 0.025 ± 0.009 dex, but based only on the analysis of iron lines.

5.3. All “hot” analogs

The whole sample of stars presented in this work is composed by 61 late F- and early G-type stars, 29 planet hosts and 32 “single” stars. In Fig. 5 we display the mean abundance difference, $\Delta[X/Fe]_{\text{SUN-STARS}}$, versus the condensation temperature,

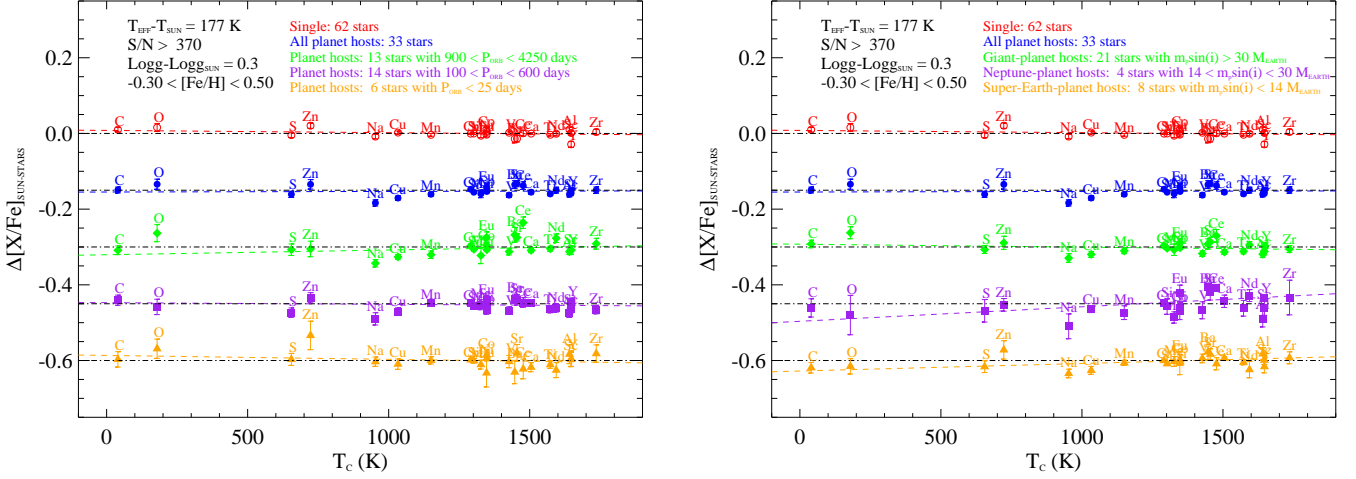


Fig. 7. *Left panel:* Same as right panel in Fig. 5 but for solar analogs containing 62 “single” stars (red open circles) and 33 stars hosting planets (blue filled circles), with the most massive planet in an orbital period $P_{\text{orb}} < 25$ days (6 stars, yellow filled triangles), $100 < P_{\text{orb}} < 600$ days (14 stars, violet filled squares), $900 < P_{\text{orb}} < 4250$ days (13 stars, green filled triangles). The mean abundance differences, $\Delta[X/H]_{\text{SUN-STARS}}$, and linear fits have been artificially shifted by -0.15 dex, for the sake of clarity. Horizontal dashed-dot lines show the zero point levels for each set of points. *Right panel:* Same as left panel but for planet-host stars with the minimum mass of the least massive planet in the ranges: $m_p \sin i < 14 M_{\oplus}$ (8 stars, yellow filled triangles), $14 < m_p \sin i < 30 M_{\oplus}$ (4 stars, violet filled squares), $m_p \sin i > 30 M_{\oplus}$ (21 stars, green filled triangles).

T_c , using the HARPS spectrum⁶ of *Ganymede* as solar reference (see González Hernández et al. 2010, for further details). The left panel of Fig. 5 evinces a high scatter among the points for different elements for both stars with and without planets and therefore, the fits are very tentative and do not provide any additional information. However, the fact that, in this relatively narrow metallicity range, the Galactic trends shown in Figs. 2, 3 and 4 give different slopes, is strongly affecting the mean element abundance ratios. For this reason, we also compute the values $\Delta[X/Fe]_{\text{SUN-STARS}}$ but after subtracting these Galactic evolution effects. To do that, we fit a linear function to the Galactic trends of the 32 “hot” analogs without planets (see linear fits in Figs. 2, 3 and 4) and subtract the value given by this fit at the metallicity of each star to the abundance ratio of the star.

The result is depicted in the right panel of Fig. 5. For “single” stars, the mean abundance ratios of practically all elements become roughly zero, with a tiny scatter ($\sigma = 0.0097$), as well as the slope of the fit to all mean abundances is almost null, with a value of $(-0.09 \pm 0.04) \times 10^{-4}$ dex K^{-1} . For “hot” analogs hosting planets, the remaining scatter is larger and thus the slope of the fit keeps still negative, $(-0.24 \pm 0.05) \times 10^{-4}$ dex K^{-1} (see Table 4). This is probably due to the fact that we are using the linear fits to the Galactic trends of stars without planets, although the abundance ratios of planet hosts seem to follow the Galactic trends defined by these linear fits. However, if we choose planet hosts to fit their galactic chemical trends the result give a similar scatter ($\sigma = 0.0121$) as the that that abundance ratios of “single” stars in Fig. 5, and the fit is almost null (-0.013 ± 0.046) . Hereafter we use abundance ratios of “single” stars to fit the Galactic trends because they cover the whole range of metallicity whereas planet hosts mostly cover metallicities $[Fe/H] > 0$, thus “single” stars are better tracers of Galactic chemical evolution effects.

This may be also due to intrinsic differences between the abundance pattern of stars with and without planets, a possibility that we will explore in Section 5.7. This could be also related to the different metallicity distribution of stars with and without planets, being the former more metal-rich, but as we will see in Section 5.4, a sub-sample of metal-rich “hot” analogs without planets still behaves in a different way that a similar sample of stars with planets.

5.4. Metal-rich “hot” analogs

We selected a sub-sample of 26 metal-rich “hot” analogs with the aim of investigating the abundance pattern of similar samples of stars with and without planets with very similar metallicity distribution. Thus, we selected 13 planet-host and 13 “single” late F- and early G-type stars. In Fig. 6 we display the mean values $\Delta[X/Fe]_{\text{SUN-STARS}}$ for these two sub-samples. In the left panel of Fig. 6, again planet hosts yield a steeper abundance trend versus condensation temperature than “single” hot analogs. However, in the right panel of Fig. 6, after removing the chemical evolution effects, the abundance pattern of “single” stars does not exhibit any trend whereas for planet hosts the mean abundances still hold a negative slope.

Meléndez et al. (2009) and Gonzalez et al. (2010); Gonzalez (2011) found that the planet-host stars show steeper trends than “single” stars at high metallicity although this effect is probably related to chemical evolution effects. González Hernández et al. (2011a) depicted in their Fig. 3 the mean abundance trends of a sub-sample of metal-rich solar analogs with and without planets together with steep fits to the data, but with similar slopes in both cases, $(-0.23 \pm 0.06) \times 10^{-4}$ dex K^{-1} for “single” stars and $(-0.16 \pm 0.05) \times 10^{-4}$ dex K^{-1} for planet-host stars (see also González Hernández et al. 2010). They display however in their Fig. 4 that after removing the galactic chemical evolution effects, these negative trends almost disappear and clearly the slopes of stars with and without planets are consistent within the $1-\sigma$ uncertainties, $(-0.07 \pm 0.06) \times 10^{-4}$ dex K^{-1} for “sin-

⁶ The HARPS solar spectra can be downloaded at <http://www.eso.org/sci/facilities/lasilla/instruments/harps/inst/monitoring/sun.html>

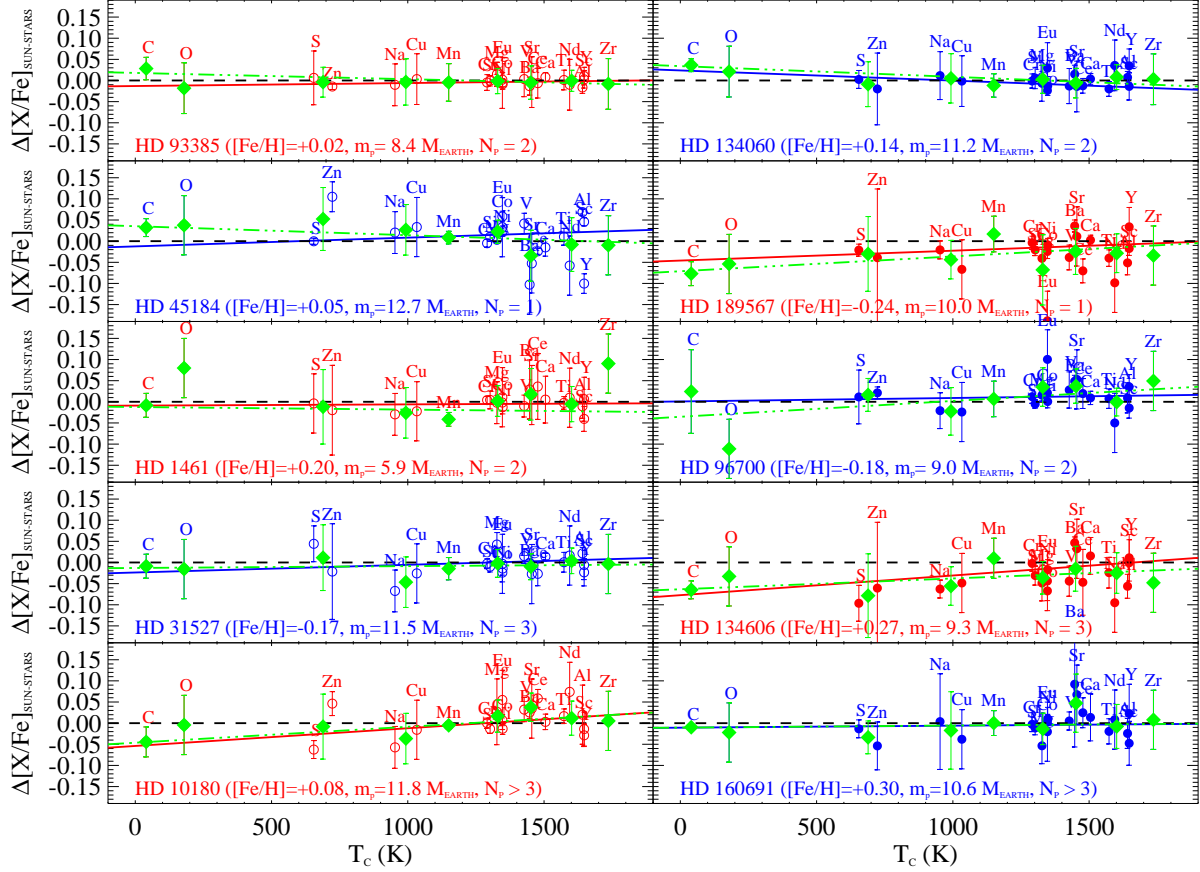


Fig. 8. Abundance differences, $\Delta[X/Fe]_{\text{SUN-STARS}}$, between the Sun and 10 stars hosting super-Earth-like planets (circles), 2 corresponding to the sample of “hot” analogs (top panels) and 8 belong to the sample of solar analogs analyzed in González Hernández et al. (2010). Error bars are the uncertainties of the element abundance measurements, corresponding to the line-by-line scatter. Diamonds show the average abundances in bins of $\Delta T_c = 150$ K. Error bars are the standard deviation from the mean abundance of the elements in each T_c bin. Linear fits to the data points (solid line) and to the mean data points (dashed-dotted line) weighted with the error bars are also displayed.

gle” stars and $(-0.02 \pm 0.05) \times 10^{-4}$ dex K^{-1} for planet-host stars (see Table 4). In addition, the mean abundance pattern of solar analogs after correcting for galactic chemical evolution exhibit also flat trends for the 62 “single” stars and 33 planet hosts (González Hernández et al. 2013b). On the other hand, if one chooses a sub-sample of very high quality spectra of metal-rich “hot” analogs with $S/N > 550$, then although the trends still remain very steep with negative slopes, in this case, for 10 stars with and 10 without planets (González Hernández et al. 2013a), these slopes are both very similar and consistent within the error bars (see Table 4).

5.5. Revisiting solar analogs

The number of planet hosts in the sample of solar analogs in González Hernández et al. (2010) have changed due to the discovery of planets of different masses, in particular, low-mass planets with masses below $30 M_{\oplus}$ (see e.g. Mayor et al. 2011). We have reanalyzed the data presented in González Hernández et al. (2010), and we have been able to correct the abundance differences, $\Delta[X/Fe]_{\text{SUN-STARS}}$, for the chemical evolution effects using the linear fits to the Galactic abundance ratios, $[X/Fe]$, of solar analogs without known planets.

In Fig. 7 we display the mean abundance differences for updated list of stars with and without detected planets. Stars hosting planets are also separated for different orbital periods of the most massive planet in the planetary systems. However, we do not see any clear signature. All of them show similar mean abundance pattern although with slightly different slopes, as those found for the whole samples of stars with and without planets. However, one could speculate that the positive trend seen for the largest orbital periods ($P_{\text{orb}} > 900$ days) would allow the formation of terrestrial planets in closer orbits. For the most massive planets at the orbital periods between 100 and 600 days, we get a flat trend (see Table 4). The stars with the most massive planets at the shortest periods ($P_{\text{orb}} < 25$ days) display a slightly negative trend, which would indicate that these stars would not have formed terrestrial planets or that they have being captured via, for instance, a possible inward migration of the most massive planet in these systems. A similar slope is found for stars without detected planets, however these slope values are only significant at $\leq 2 \sigma$ (see Table 4) which makes the previous statement probably too tentative.

In the right panel of Fig. 7, we depict the mean abundance differences but separating the planet hosts in several ranges of the minimum mass of the least massive planet. The mean abun-

Table 4. Slopes of the linear fit to the mean values $\Delta[X/Fe]_{\text{SUN-STARS}}$ versus T_C

Sample ^a	Non-GCE ^b	GCE ^b	N_{stars}^c
sSA	-0.378 ± 0.033	-0.060 ± 0.029	62
pSA	-0.302 ± 0.047	$+0.014 \pm 0.040$	33
smrSA	-0.235 ± 0.055	-0.062 ± 0.053	16
pmrSA	-0.194 ± 0.048	-0.027 ± 0.047	16
sHA	-0.160 ± 0.046	-0.086 ± 0.041	32
pHA	-0.404 ± 0.048	-0.242 ± 0.046	29
smrHA	-0.111 ± 0.062	-0.106 ± 0.061	13
pmrHA	-0.506 ± 0.066	-0.379 ± 0.063	13
smrHAh	-0.330 ± 0.069	-0.258 ± 0.070	10
pmrHAh	-0.419 ± 0.068	-0.289 ± 0.067	10
pSAIp	-0.099 ± 0.067	$+0.125 \pm 0.059$	13
pSAmp	-0.370 ± 0.075	-0.044 ± 0.062	14
pSAsp	-0.404 ± 0.114	-0.103 ± 0.092	6
pSAlm	-0.348 ± 0.059	-0.077 ± 0.050	21
pSAmm	$+0.236 \pm 0.114$	$+0.383 \pm 0.097$	4
pSAsm	-0.223 ± 0.084	$+0.199 \pm 0.065$	8

Notes. Slopes of the linear fit of the mean abundance ratios, $\Delta[X/Fe]_{\text{SUN-STARS}}$, as a function of the condensation temperature, T_C , using the whole T_C interval, for different stellar samples. ^(a) Stellar samples: “single” solar analogs, “sSA”, planet-host solar analogs, “pSA”, “single” metal-rich solar analogs, “smrSA”, planet-host metal-rich solar analogs, “pmrSA”. “HA” refers to “hot” analogs and “HAh” refers to very high S/N data (S/N > 550). Planet-host solar analogs with the most massive planet in an orbital period $P_{\text{orb}} < 25$ days, “pSAsp”, $100 < P_{\text{orb}} < 600$ days, “pSAmp”, $900 < P_{\text{orb}} < 4250$ days, “pSAIp”. Planet-host solar analogs with the minimum mass, $m_p \sin i$, of the least massive planet in the ranges: $m_p < 14 M_{\oplus}$, “pSAsm”, $14 < m_p < 30 M_{\oplus}$, “pSAmm”, $m_p > 30 M_{\oplus}$, “pSAlm”. ^(b) “Non-GCE” and “GCE” refers to the mean abundances before and after being corrected for galactic chemical evolution effects. ^(c) Total number of stars in the sample.

dance patterns are similar but the slopes of the trends seem to behave in a different way depending on the range of masses. We try again to speculate on these results to try to identify possible explanations. The stars containing super-Earth-like planets show an increasing trend, which would indicate that these stars are slightly different than the Sun and that the super-Earth-like planets behave on average as the terrestrial planets of the solar planetary system, but with higher amount of metals trapped on these super-Earth-like planets. On the other hand, the stars harbouring Neptune-like planets show on average a steep positive trend slope which would mean that the Neptune-like planets have, as one may expect, a higher content of refractory elements than the Sun and the volatile content caught in Neptune-like planets would not be too large. Finally, the stars hosting Jovian planets exhibit a slightly negative or almost flat trend, which may indicate that these stars only harbour giant planets, although in that case one would expect to see a steep negative trend. There still remain the possibility that these stars harbour a small amount of terrestrial planets. The ideal situation would be to group the stars taking into account at the same time the planet mass and periods but the statistics would be even worse. Thus, these statements, although they appear to follow the line of reasoning in Meléndez et al. (2009), we think we need more Sun-like stars with already detected planets at different masses and orbital periods and with high-quality data to confirm this very tentative scenario. In the next section we individually inspect the abun-

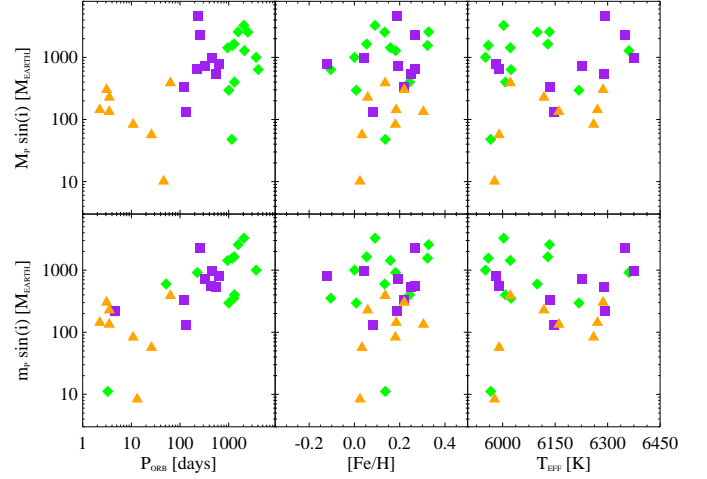


Fig. 9. *Top panels:* Minimum mass of the most massive planet of each of “hot” analogs hosting planets versus the orbital period of the planet (left panel) and metallicity [Fe/H] (middle panel), and temperature (right panel), with the most massive planet in an orbital period $P_{\text{orb}} < 65$ days (diamonds), $115 < P_{\text{orb}} < 630$ days (squares), $950 < P_{\text{orb}} < 4050$ days (triangles). *Bottom panels:* the same as top panels but showing the minimum mass of the least massive planet. The symbols as in top panel.

dance pattern of the stars hosting super-Earth-like and Neptune-like planets to try to elucidate whether there is a connection between the amount of rocky material in the low-mass planets and the slopes of the abundance trends of each star.

5.6. Stars hosting super-Earth-like planets

González Hernández et al. (2010) already studied the abundance trends of two stars in their sample, with negative slopes, which harbour super-Earth-like planets, HD 1461 and HD 160691. Taking into account the new discovered planets presented e.g. in Mayor et al. (2011), our sample of solar analogs analyzed in González Hernández et al. (2010) and our sample of “hot” analogs now contain 8 and 2 stars hosting super-Earth-like planets, respectively. It is therefore interesting to look at the abundance pattern of these stars harbouring, at least, super-Earth-like planets under the assumption that these exoplanets contain a significant amount of rocky material in form of refractory elements. We note here that the masses of the planet are indeed minimum masses and therefore in some cases the “real” planet mass could be significantly larger. However, statistical analysis show that the distribution of $m_p \sin i$ values is similar to that of “ m_p ” values Jorissen et al. (2001). In fact, the average value of $\sin i$ for a random distribution of angles is of 0.79, so the average factor of overestimation is only 1.27.

In Fig. 8 we display the abundance pattern of the only 10 stars hosting super-Earth-like planets in the sample of “hot” analogs and the sample of solar analogs analyzed in González Hernández et al. (2010). The abundance differences of these stars, $\Delta[X/Fe]_{\text{SUN-STARS}}$, are plotted versus the condensation temperature, T_C . The abundances ratios of each star were corrected for the Galactic trends at the metallicity of the star. To compute these abundance corrections we use the linear fitting functions of the galactic abundances of both the sample of 32 “hot” and 62 solar analogs without detected planets. In Fig. 8 we also show the fits to all abundance ratios of each star weighted

by their uncertainties. There are much more refractory elements (with $T_C \gtrsim 1200$ K) than volatile elements, so a more reliable fit of these element abundance ratios should consider the whole of T_C values. However, we still think that this fitting procedure does not give the same weight to all T_C values and thus we decided to average the abundance ratios in bins of $\Delta T_C = 150$ K. We estimate the error bars of these new points as the maximum value between standard deviation from the mean abundance and the mean abundance uncertainty of the elements at each T_C bin, unless in this T_C bin there is only one point, in which case, the error bar is associated with the abundance uncertainty of the given element. The error bar is estimated in this way in order to take into account all possible sources of uncertainty, i.e. not only the scatter of the element abundances but also the individual abundance uncertainties. These new data points are also depicted in Fig. 8 together with their corresponding linear fitting functions, we were again derived by the fit of these points weighted by the error bars. The slope of these linear fits is our adopted slope to be evaluated in the context of the possible presence of terrestrial planets in these stars. In many cases, these new fits of the average points are similar to those corresponding to the individual element abundances.

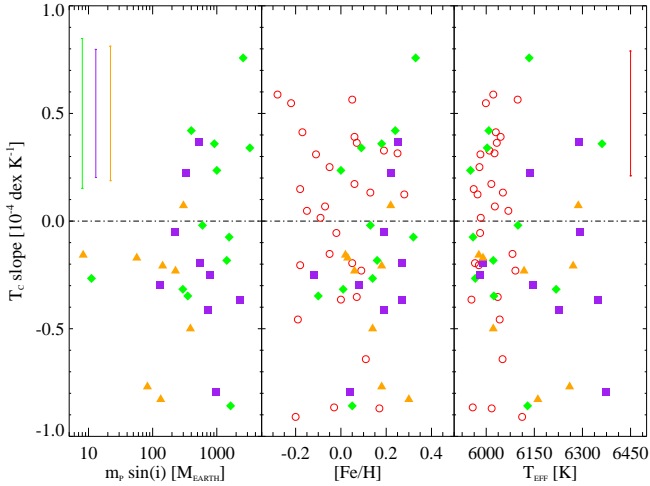


Fig. 10. Slopes of the linear fits to 61 “hot” analogs of the mean element abundance ratios, $\Delta[X/Fe]_{\text{SUN-STARS}}$, versus the condensation temperature, T_C , as a function of the minimum mass of the least massive planet of each planet-host star (left panel), the stellar metallicity (middle panel), and effective temperature (right panel). The mean error bars of the slopes are shown in upper-left corner for planet hosts and upper-right corner for “single” stars. The symbols as in Fig. 9.

By inspecting Fig. 8, one realizes that there are 4 stars showing positive slopes, 3 stars showing negative slopes and 3 stars giving a null slope. We note that if all the stars would provide a null slope, the interpretation related to the existence of terrestrial planets would lose its meaning. Anyway, the magnitude of the slope should in principle be related to the amount of rocky material present in these planetary systems. Thus, finding one single planetary system that does not accomplish the expected slope may be enough to rule out the statement claiming that the abundance pattern of a star conceal a signature of rocky planets. In these small sub-sample of 10 stars hosting small planets, there are 3 stars providing negative trends, but having relatively massive super-Earth-like planets. In these 3 stars, one would expect

to find, at least, similar positive trends as for other stars in this small sub-sample. However, we still do not know if these stars actually harbour really rocky Earth-like planets.

In Fig. 8 we also indicate the number of confirmed planets in these planetary systems. It does not seem to be any connection between the number of planets and the slope of the abundance pattern versus condensation temperature. The solar analogs with only two detected planets, HD 1461 and HD 96700, whose less massive planet has 5.9 and 9.0 M_{\oplus} at an orbital period $P_{\text{orb}} \sim 13.5$ and 8.1 days, respectively, and have a second super-Earth-like planet with a 7.6 and 12.7 M_{\oplus} (at $P_{\text{orb}} \sim 5.8$ and 103.5 days), respectively, and hence a significant amount of rocky material. Nevertheless, they both exhibit unexpected nearly flat trends. In addition, the two “hot” analogs, with $T_{\text{eff}} \sim 5975$ K, should have narrower convective zones than the Sun what would make it easier to detect any possible signature of terrestrial planets. These two stars, HD 93385 and HD 134060, harbour two planets each with masses 8.4 and 10.2 (at $P_{\text{orb}} \sim 13.2$ and 46 days) and 11.2 and 47.9 M_{\oplus} (at $P_{\text{orb}} \sim 3.2$ and 1160.9 days). These planets should also contain a large amount of rocky material and hence refractory elements but they have slightly lower volatile-to-refractory abundance ratios than the Sun, and therefore should have less amount of rocky material than that of the solar planetary system.

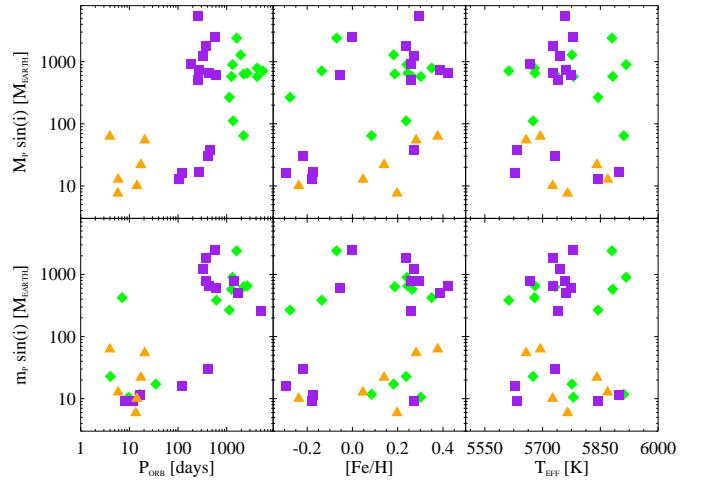


Fig. 11. Same as Fig. 9, but for solar analogs hosting planets, with the most massive planet in an orbital period $P_{\text{orb}} < 25$ days (diamonds), $150 < P_{\text{orb}} < 650$ days (squares), $1000 < P_{\text{orb}} < 4300$ days (triangles).

It is actually plausible that many of our stars in both samples of “hot” and solar analogs host really terrestrial planets. Numerical simulations reveal that low-mass (from Neptune-like to Earth-like) planets are much more common than giant planets, and this effect is more significant as the metallicity decreases, and probably 80–90% of solar-type stars have terrestrial planets (see e.g. Mordasini et al. 2009a,b, 2012). This statement agrees with the growing population of low mass planets found in the HARPS sample of exoplanets (Udry & Santos 2007; Howard et al. 2010; Mayor et al. 2011).

5.7. Planetary Signatures in the Abundance Trends?

We now explore the abundance trends of the whole sample of “hot” and solar analogs to extract information on the amount of

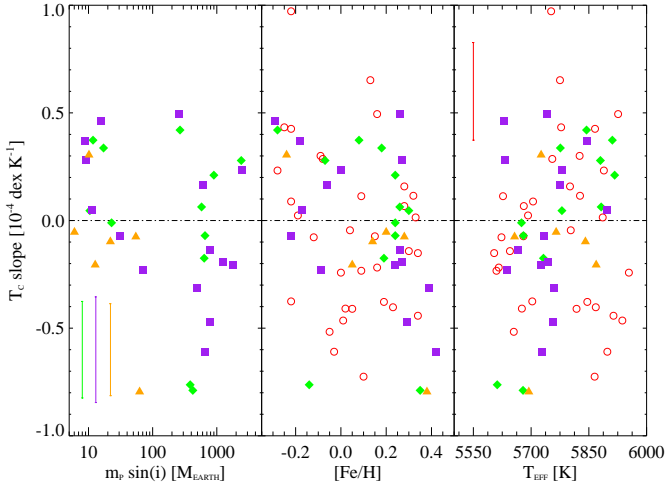


Fig. 12. Same as Fig. 10 but for solar analogs. The symbols as in Fig. 11.

rocky material in their planetary systems. In Fig. 9 we depict the important orbital properties, minimum mass of the most massive and the least massive planets, and the orbital period as well as two stellar properties, metallicity and effective temperature, of all the 29 “hot” analogs with planets. Fig. 9 exhibits a variety of planetary systems, many of them with more than one or two planets. This plot also allows us to see that there are only two stars hosting super-Earth-like planets (see also Fig. 8) with $T_{\text{eff}} \sim 5975$ K and metallicities slightly above solar, but also that the most massive planets in these systems are another Super-Earth-like and one Saturn-like planet in about 6- and 100-day orbits (see Section 5.6). In Fig. 9 we are also able to distinguish many stars harbouring isolated planets, with masses between 50 and $3500 M_{\oplus}$. The stellar properties of the stars, T_{eff} and $[\text{Fe}/\text{H}]$, exhibit an uniform behaviour irrespective for the orbital period of the most and the least massive planet in each planetary system.

Although the planetary systems of the sample of “hot” analogs exhibits a substantial complexity, we try to extract information from the slopes of the average abundances versus the condensation temperature as seen in Section 5.6. Thus we derive the trend of the average abundances in T_C bins of each “hot” analogs as shown for the stars hosting super-Earth-like planets in Fig. 8. In Fig. 10 we depict the slopes of these average trends as a function of the minimum mass of the least planet mass, and stellar metallicity and effective temperature. We also display the slopes for “hot” analogs without known planets. According to the line of reasoning in Meléndez et al. (2009), positive slopes would mean that these stars are deficient in refractory elements with respect to the sun and hence likely to host terrestrial planets. From this plot one realize that only a few stars which already harbour giant planets would also have terrestrial planets. However, most of the “hot” analogs, in particular, two stars that already contains super-Earth-like planets exhibit negative slopes, and hence with less probability of hosting terrestrial planets. We also include stars without known planets and more than half of them seem to better accommodate in positive slopes and therefore having terrestrial planets.

In Fig. 11, we display the minimum masses of the planets orbiting 33 solar analogs similarly as in Fig. 9. We notice here that there are 8 solar analogs with Super-Earth-like planets with masses between 6 and $13 M_{\oplus}$ at orbital periods between 6 and 16 days, and 4 Neptune-like planets, with masses 16 and $23 M_{\oplus}$ at

P_{orb} in the range 4–122 days. The distributions of effective temperatures and metallicities among solar analogs are also approximately homogeneous and do not depend on the orbital period of the planets. In Fig. 12, we depict the slopes for solar analogs with and without planets computed as in Fig. 10. We also display the mean error bars for different samples of stars with and without planets to illustrate how accurate are these slopes. In fact, many of these values are consistent with null slopes. We see that among stars with low-mass planets, many of them exhibit positive slopes. Most of these planetary systems have Jupiter-like or Saturn-like planet at orbital periods longer than 100 days. On the other hand, the two solar analogs, showing negative slopes, only harbour Super-Earth-like planets at orbital periods shorter than 25 days. Solar-type stars with only giant planets at long orbital period display mostly negative slopes, which may indicate that they do not host terrestrial planets, although there are some with positive slopes. The solar analogs without detected planets are roughly equally distributed above and below the null slope.

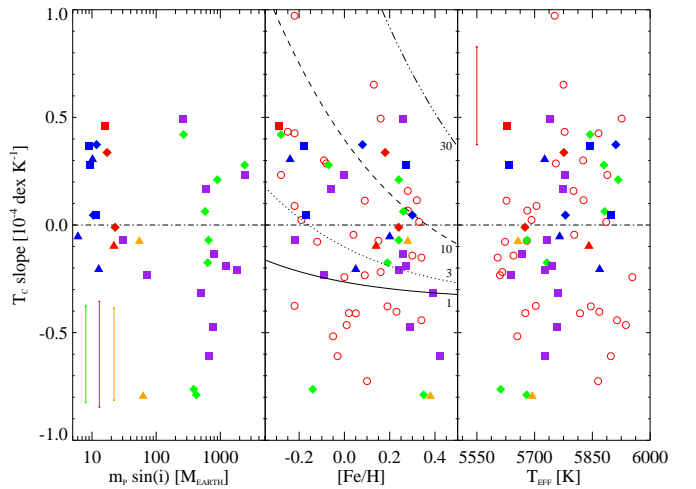


Fig. 13. Same as Fig. 12 but highlighting stars with super-Earth-like planets (red filled symbols) and stars with Neptune-like planets (blue filled symbols). The predicted lines (black lines) tracking the amount of rocky material in the planetary systems as 1, 3, 10, and $30 M_{\oplus}$.

Chambers (2010) demonstrated that is possible to explain the abundances of solar twins in Meléndez et al. (2009) by adding 4 Earth masses of rocky material. In the solar system, the terrestrial planets only have about $2 M_{\oplus}$ of rock. However, the primordial asteroid belt probably contained a similar amount of rocky protoplanets (Weidenschilling 1977). This mass of rock was probably ejected from the solar system once Jupiter formed (see e.g. Chambers & Wetherill 2001), and thus would be missed from the solar photosphere. Therefore, the existence of the present terrestrial planets and the asteroid belt in the solar planetary system could explain the abundance pattern of the solar twins with respect to the Sun. Chambers (2010) argued that just adding $4 M_{\oplus}$ of Earth-like material to the current solar photosphere is enough to sufficiently increase the amount of refractory elements but not to reproduce the abundance pattern of solar twins in Meléndez et al. (2009). In order to approximately recover that pattern one needs to add $4 M_{\oplus}$ of a equal mixture of Earth-like and CM chondrite material, but provided that the fractionation is limited to the current size of the convection zone, which comprises $\sim 2.5\%$ of the Sun’s mass. Thus, this

augmented solar abundance pattern roughly matches the mean abundance of those solar twins both for volatile and refractory elements, suggesting that the Sun could have accreted refractory-poor material from both the terrestrial-planet and the asteroid-belt regions (Chambers 2010).

One of the problems of this simple model is probably the size of the convection zone at the time of the formation of terrestrial planets. This issue was already discussed in Meléndez et al. (2009) where they already pointed out that protoplanetary disks have typical lifetimes $\lesssim 10$ Myr (see e.g. Sicilia-Aguilar et al. 2006; Mordasini et al. 2012), but at that time, the mass fraction of the convection zone of a solar-type star is about 40 % (D’Antona & Mazzitelli 1994), and it goes down to its current size likely after 30 Myr. However, recently Baraffe & Chabrier (2010) have shown that episodic accretion during pre-main-sequence evolution of solar-mass stars could yields quicker reach of the current size convection zone as the initial mass, before the onset of the accretion episodes, of the protostars decreases. Thus, only in the case of initial mass of the protostars before the onset of the accretion bursts as low as $10 M_{\text{Jup}}$ (with accretion rates of $0.5 M_{\text{Jup}} \text{ yr}^{-1}$ during episodes lasting for 100 yr), the convection zone would reach the current size in about 6-8 Myr, and therefore consistent with the lifetime of the protoplanetary disk in the above scenario. Different efficiencies of episodic accretion and also the composition of the accreted material may also affect the final atmospheric abundances of the star.

On the other hand, the accretion of small planets containing “heavy” refractory elements, that may happen for instance during inward migration of massive planets (as mentioned in section 5.5), may also affect the composition of the convective zone of these stars depending on the relative strength of thermohaline mixing/convection the μ -gradient, external turbulence, radiative levitation, and rotation-induced mixing (see Vauclair & Théado 2012, and references therein). The remaining question may be how much this affects the accretion of volatiles elements like C, N, and O during accretion of dust-depleted gas needed to explain the solar abundances in the above scenario.

Giant planets of the solar system also contain a significant amount of refractory elements, $\sim 50 - 100 M_{\oplus}$ (Guillot 2005), but they do not appear to be enriched in rock-forming elements compared to ices (Owen et al. 1999). Thus, it is difficult to estimate how much giant-planet formation can affect the photospheric abundances of refractory elements in solar-type stars (see the discussion in Chambers 2010, for more details).

Chambers (2010) elaborated a simple model which quantifies the amount of rocky material in a stars’ planetary system from the slopes of the trends described by the abundance ratios of a sample of solar analogs versus the condensation temperature, T_C . They use the slopes derived by to tentatively identify stars harbouring terrestrial planets, according to their model. We have applied this model to our sample of solar analogs, but we use the slopes determined using the average abundances in bins of $\Delta T_C = 150$ K as described in Section 5.6 and displayed in Fig. 12. We use both equations 1 and 2 in Chambers (2010) to estimate the mass of the accreted fractionated material, M_{frac} , which is mixed with material in the stellar convective zone, M_{CZ} , and the mass of rocky material, M_{rock} . We assume the mass of convective zone to be constant over time and equal to $0.02 M_{\odot}$ for all solar analogs (Pinsonneault et al. 2001). We also adopt the whole interval of condensation temperature 40–1750 K. We choose as minimum slope, which corresponds to the parameter S_{max} in Chambers (2010), the value

of $-0.35 \times 10^{-4} \text{ dex K}^{-1}$, since most of the points are above this value.

In Fig. 13, we depict the same plot as Fig. 12, but highlighting those stars hosting super-Earth-like, with minimum masses, $m_p \sin i$, between 5 and $14 M_{\oplus}$, and Neptune-like, with $m_p \sin i$ 14– $30 M_{\oplus}$, planets. In the middle panel of Fig. 13 we also display lines corresponding to the amount of rocky material which is expected to be missed from the atmosphere of the stars according to their slopes. These lines should track the amount of mass which is into terrestrial planets, maybe also Super-Earth-like planets, as well as possible asteroid belts. This plot is similar to Figure 3 in Chambers (2010), but the values used by Chambers (2010) are larger mainly due to the fact that we subtract the chemical evolution effects from abundance trends of the stars, and Ramírez et al. (2009) did not. In addition, in this plot we distinguish among stars with and without known planets and different minimum masses of the planets, being super-Earth-like, Neptune-like and giant planets. We note that we assume that at least super-Earth-like planets should contribute to the amount of missing rocky material from the stellar atmospheres. The position of the zero point depends on the adopted minimum slope, so we may only considered these lines as a tentative indication of possible amount of terrestrial planets in the planetary systems of these solar analogs. This is probably a weak point of this simple model, which may only prevent us to extract strong conclusions from this comparison. However, using this value we are able to roughly reproduced the amount of rocky material in the solar planetary system, $M_{\text{rock}} \sim 4 M_{\oplus}$, which gives a null slope at $[\text{Fe}/\text{H}] = 0$.

Fig. 13 reveals that most of the stars may host certain amount (more than $3 M_{\oplus}$) of terrestrial planets. In particular, between 3 and $10 M_{\oplus}$ there are many stars with already detected super-Earth-like planets, but there is no clear correlation between the slope values and amount of missing rocky material. Stars with known super-Earth-like planets with similar mass have in some cases very different predicted missing masses of rock. Thus, for instance, the star HD 45184 with only one super-Earth-like planet at $\sim 13 M_{\oplus}$ exhibits negative slope but the predicted amount of rocky materials is $\sim 2 M_{\oplus}$. The slope of the star HD 1461, which has two super-Earth-like planets accounting for at total mass of $\sim 14 M_{\oplus}$, yields a mass of rock of $\sim 6 M_{\oplus}$. The two stars with nearly null slopes at about $+0.05 \times 10^{-4} \text{ dex K}^{-1}$, HD 31527 and HD 160691, and with low-mass planets at about $\sim 11 M_{\oplus}$, have however very different predicted rocky masses, at ~ 3 and $\sim 10 M_{\oplus}$, respectively. This may mean that super-Earth-like planets are not traces of rocky missing material but only Earth-like planets, or that the assumption that the slope of abundance trends versus condensation temperature are not related with the amount of terrestrial planets in the planetary systems of solar analogs.

In Fig. 13 we also depict stars with Neptune-like planets, which may also hold rocky cores covered by volatile-rich atmospheres. Similarly we do not really know if super-Earth-like planets have an atmosphere or a crust rich in volatiles. Two stars with $\sim 17 M_{\oplus}$, have however significantly different predicted missing mass of rock from the stars’ atmosphere at roughly 7 and $14 M_{\oplus}$. The size of the cores of these two planets are unknown but if we assume that the cores are similar, then the star at higher metallicity may also harbour some undetected Earth-like planets. However, again we cannot prove this is the case but we cannot also demonstrate either that the reasoning in Meléndez et al. (2009); Ramírez et al. (2009) is correct.

5.8. Conclusions

We have explored in the HARPS database to search for main-sequence stars with hotter effective temperature than the Sun and selected a sample in the T_{eff} range 5950–6400 K of 32 “single” stars and 29 stars hosting planets with high-resolution ($\lambda/\delta\lambda \gtrsim 85,000$) and very high signal-to-noise ($S/N \gtrsim 250$ and $S/N \sim 800$ on average) HARPS, UVES and UES spectroscopic data. We have tried to evaluate the possible connection between the abundance pattern versus the condensation temperature, T_C , and the presence of terrestrial planets.

We perform a detailed chemical abundance analysis of this sample of “hot” analogs and investigate possible trends of mean abundance ratios, $\Delta[X/\text{Fe}]_{\text{SUN-STARS}}$, versus T_C , after removing the Galactic chemical evolution effects. We find that both stars with and without planets show a similar mean abundance pattern with slightly negative slopes. We also analyze a sub-sample of metal-rich “hot” analogs in the narrow metallicity range $+0.04$ – $+0.19$ and find also negative slopes for both stars without and with planets, and almost equal mean abundance patterns when restricting the sample to very high quality spectra ($S/N > 550$).

We also revisit the sample of solar analogs in González Hernández et al. (2010) with the updated number of planet hosts, 62 “single” stars and 33 stars with planets. We investigate the mean abundance pattern of solar analogs harbouring planets with the most massive planets at different orbital periods and with the least massive planet being a super-Earth-like, a Neptune-like and a Jupiter-like planet. We speculate within the scenario in which the presence of rocky planets affect the volatile-to-refractory abundance ratios in the atmosphere of these planet-host stars. In each case the slope value reveals expected value according to this scenario, assuming that the bulk chemical composition of super-Earth-like planets is closer to the Earth composition than that of Neptune-like and Jovian planets.

This sample of solar analogs and that of “hot” analogs have a sub-sample of 8 and 2 stars harbouring super-Earth-like planets. We compute the average abundance ratios $\Delta[X/\text{Fe}]_{\text{SUN-STARS}}$ versus condensation, T_C , in bins of $\Delta T_C = 150$ K, and individually fit these abundances to get the slope of the average abundance pattern of each star. We find that only four stars show positive abundance trends, qualitatively in agreement with the expected value according to the reasoning in Meléndez et al. (2009); Ramírez et al. (2009). However, three stars show nearly null slopes and three stars exhibit unexpected negative trends since they harbour super-Earth-like planets.

Finally, we derive the slopes of the trend $\Delta[X/\text{Fe}]_{\text{SUN-STARS}}$ versus T_C for each star of the whole sample of solar analogs and compare them with a simple model of the amount of rocky material missed in the stars’ atmospheres. Several solar analogs containing super-Earth-like planets of typically $m_p \sin i \sim 11 M_{\oplus}$, with different slopes, provide very non-consistent predictions of the missing amount of rocks, from 2 to $15 M_{\oplus}$. This might mean that only Earth-like planets could track the amount of missing rocky material in the atmospheres of solar analogs. Therefore, this comparison cannot provide a clear evidence that in the abundance pattern of a solar-type star there exist hints of the presence of terrestrial planets in the planetary system of each star.

Acknowledgements. J.I.G.H. and G.I. acknowledge financial support from the Spanish Ministry project MICINN AYA2011-29060 and J.I.G.H. also from the Spanish Ministry of Science and Innovation (MICINN) under the 2009 Juan de la Cierva Programme. This work was also supported by the European Research Council/European Community under the FP7/EC through a Starting Grant agreement number 239953, as well as by Fundação para a Ciência e Tecnologia (FCT)

in the form of grant reference PTDC/CTE-AST/098528/2008. N.C.S. would further like to thank FCT through program Ciência 2007 funded by FCT/MCTES (Portugal) and POPH/FSE (EC). V.Zh.A. and S.G.S. are supported by grants SFRH/BPD/70574/2010 and SFRH/BPD/47611/2008 from FCT (Portugal), respectively. E.D.M. is supported by grant SFRH/BPD/76606/2011 from FCT (Portugal). This research has made use of the SIMBAD database operated at CDS, Strasbourg, France. This work has also made use of the IRAF facility, and the Encyclopaedia of extrasolar planets.

References

- Adibekyan, V. Z., Delgado Mena, E., Sousa, S. G., et al. 2012a, *A&A*, 547, A36
 Adibekyan, V. Z., Santos, N. C., Sousa, S. G., et al. 2012b, *A&A*, 543, A89
 Adibekyan, V. Z., Sousa, S. G., Santos, N. C., et al. 2012c, *A&A*, 545, A32
 Allende Prieto, C., Lambert, D. L., & Asplund, M. 2001, *ApJ*, 556, L63
 Baraffe, I. & Chabrier, G. 2010, *A&A*, 521, A44
 Bensby, T., Feltzing, S., Lundström, I., & Ilyin, I. 2005, *A&A*, 433, 185
 Bond, J. C., O’Brien, D. P., & Lauretta, D. S. 2010, *ApJ*, 715, 1050
 Buchhave, L. A., Latham, D. W., Johansen, A., et al. 2012, *Nature*, 486, 375
 Carter-Bond, J. C., O’Brien, D. P., Delgado Mena, E., et al. 2012a, *ApJ*, 747, L2
 Carter-Bond, J. C., O’Brien, D. P., & Raymond, S. N. 2012b, *ApJ*, 760, 44
 Chambers, J. E. 2010, *ApJ*, 724, 92
 Chambers, J. E. & Wetherill, G. W. 2001, *Meteoritics and Planetary Science*, 36, 381
 D’Antona, F. & Mazzitelli, I. 1994, *ApJS*, 90, 467
 Delgado Mena, E., Israelian, G., González Hernández, J. I., et al. 2010, *ApJ*, 725, 2349
 Ecuivillon, A., Israelian, G., Santos, N. C., Mayor, M., & Gilli, G. 2006, *A&A*, 449, 809
 Gilli, G., Israelian, G., Ecuivillon, A., Santos, N. C., & Mayor, M. 2006, *A&A*, 449, 723
 Gonzalez, G. 2011, *MNRAS*, 416, L80
 Gonzalez, G., Carlson, M. K., & Tobin, R. W. 2010, *MNRAS*, 407, 314
 González Hernández, J. I., Delgado-Mena, E., Sousa, S. G., et al. 2013a, in *AN*, Vol. 334, *Astron. Nachr.*, ed. –, –
 González Hernández, J. I., Delgado-Mena, E., Sousa, S. G., et al. 2013b, in *ASP Conference Series*, ed. –, *Astronomical Society of the Pacific*, –
 González Hernández, J. I., Israelian, G., Santos, N. C., et al. 2010, *ApJ*, 720, 1592
 González Hernández, J. I., Israelian, G., Santos, N. C., et al. 2011a, in *Highlights of Spanish Astrophysics VI*, ed. M. R. Zapatero Osorio, J. Gorgas, J. Maíz Apellániz, J. R. Pardo, & A. Gil de Paz, 576–582
 González Hernández, J. I., Israelian, G., Santos, N. C., et al. 2011b, in *IAU Symposium*, Vol. 276, *IAU Symposium*, ed. A. Sozzetti, M. G. Lattanzi, & A. P. Boss, 422–423
 Guillot, T. 2005, *Annual Review of Earth and Planetary Sciences*, 33, 493
 Howard, A. W., Marcy, G. W., Johnson, J. A., et al. 2010, *Science*, 330, 653
 Jorissen, A., Mayor, M., & Udry, S. 2001, *A&A*, 379, 992
 Kargel, J. S. & Lewis, J. S. 1993, *Icarus*, 105, 1
 Kurucz, R. 1993, *ATLAS9 Stellar Atmosphere Programs and 2 km/s grid*. Kurucz CD-ROM No. 13. Cambridge, Mass.: Smithsonian Astrophysical Observatory, 1993., 13
 Kurucz, R. L., Furenlid, I., Brault, J., & Testerman, L. 1984, *Solar flux atlas from 296 to 1300 nm*
 Lambert, D. L. 1978, *MNRAS*, 182, 249
 Laws, C. & Gonzalez, G. 2001, *ApJ*, 553, 405
 Lodders, K. 2003, *ApJ*, 591, 1220
 Lovis, C., Ségransan, D., Mayor, M., et al. 2011, *A&A*, 528, A112
 Marcy, G., Butler, R. P., Fischer, D., et al. 2005, *Progress of Theoretical Physics Supplement*, 158, 24
 Mayor, M., Marmier, M., Lovis, C., et al. 2011, *ArXiv e-prints*
 Mayor, M., Pepe, F., Queloz, D., et al. 2003, *The Messenger*, 114, 20
 Mayor, M. & Udry, S. 2008, *Physica Scripta Volume T*, 130, 014010
 Mayor, M., Udry, S., Lovis, C., et al. 2009, *A&A*, 493, 639
 Meléndez, J., Asplund, M., Gustafsson, B., & Yong, D. 2009, *ApJ*, 704, L66
 Meléndez, J., Bergemann, M., Cohen, J. G., et al. 2012, *A&A*, 543, A29
 Mordasini, C., Alibert, Y., & Benz, W. 2009a, *A&A*, 501, 1139
 Mordasini, C., Alibert, Y., Benz, W., Klahr, H., & Henning, T. 2012, *A&A*, 541, A97
 Mordasini, C., Alibert, Y., Benz, W., & Naef, D. 2009b, *A&A*, 501, 1161
 Neves, V., Santos, N. C., Sousa, S. G., Correia, A. C. M., & Israelian, G. 2009, *A&A*, 497, 563
 Owen, T., Mahaffy, P., Niemann, H. B., et al. 1999, *Nature*, 402, 269
 Pinsonneault, M. H., DePoy, D. L., & Coffee, M. 2001, *ApJ*, 556, L59
 Ramírez, I., Asplund, M., Baumann, P., Meléndez, J., & Bensby, T. 2010, *A&A*, 521, A33
 Ramírez, I., Meléndez, J., & Asplund, M. 2009, *A&A*, 508, L17

- Ramírez, I., Meléndez, J., Cornejo, D., Roederer, I. U., & Fish, J. R. 2011, *ApJ*, 740, 76
- Reddy, B. E., Lambert, D. L., & Allende Prieto, C. 2006, *MNRAS*, 367, 1329
- Santos, N. C., Israelian, G., & Mayor, M. 2001, *A&A*, 373, 1019
- Santos, N. C., Israelian, G., & Mayor, M. 2004, *A&A*, 415, 1153
- Schuler, S. C., Cunha, K., Smith, V. V., et al. 2011a, *ApJ*, 737, L32
- Schuler, S. C., Flateau, D., Cunha, K., et al. 2011b, *ApJ*, 732, 55
- Sicilia-Aguilar, A., Hartmann, L., Calvet, N., et al. 2006, *ApJ*, 638, 897
- Snedden, C. A. 1973, PhD thesis, THE UNIVERSITY OF TEXAS AT AUSTIN.
- Sousa, S. G., Santos, N. C., Israelian, G., Mayor, M., & Monteiro, M. J. P. F. G. 2007, *A&A*, 469, 783
- Sousa, S. G., Santos, N. C., Israelian, G., Mayor, M., & Udry, S. 2011, *A&A*, 533, A141
- Sousa, S. G., Santos, N. C., Mayor, M., et al. 2008, *A&A*, 487, 373
- Takeda, Y. 2005, *PASJ*, 57, 83
- Takeda, Y. 2007, *PASJ*, 59, 335
- Udry, S., Mayor, M., Benz, W., et al. 2006, *A&A*, 447, 361
- Udry, S. & Santos, N. C. 2007, *ARA&A*, 45, 397
- Valencia, D., O'Connell, R. J., & Sasselov, D. D. 2007a, *ApJ*, 670, L45
- Valencia, D., Sasselov, D. D., & O'Connell, R. J. 2007b, *ApJ*, 665, 1413
- Valenti, J. A. & Fischer, D. A. 2005, *ApJS*, 159, 141
- Vauclair, S. & Théado, S. 2012, *ApJ*, 753, 49
- Weidenschilling, S. J. 1977, *Ap&SS*, 51, 153

Appendix A: Chemical abundance ratios [X/Fe]

In this appendix we provide all the tables containing the element abundance ratios [X/Fe] of with 32 F-, G-type stars without planets and 29 F-, G-type stars hosting planets which are all available online.

Table A.1. Abundance ratios [X/Fe] of F-, G-type analogs with planets

HD	[C/Fe]	[O/Fe]	[S/Fe]	[Na/Fe]	[Mg/Fe]	[Al/Fe]
10647	–	0.112 ± 0.070	–0.058 ± 0.042	–0.078 ± 0.057	–0.063 ± 0.064	–0.148 ± 0.014
108147	–0.131 ± 0.028	–0.181 ± 0.070	–0.136 ± 0.007	–0.051 ± 0.057	–0.041 ± 0.057	–0.116 ± 0.007
117618	–0.060 ± 0.049	–0.003 ± 0.070	–0.008 ± 0.049	0.057 ± 0.042	0.002 ± 0.021	–0.018 ± 0.021
121504	–0.112 ± 0.042	0.014 ± 0.070	–0.061 ± 0.120	–0.126 ± 0.085	–0.071 ± 0.049	–0.051 ± 0.035
134060	–0.070 ± 0.015	–0.027 ± 0.070	–0.052 ± 0.021	0.023 ± 0.057	–0.027 ± 0.042	–0.037 ± 0.014
169830	–0.018 ± 0.068	0.068 ± 0.070	–0.027 ± 0.092	0.048 ± 0.057	–0.037 ± 0.021	–0.097 ± 0.021
17051	–	–0.061 ± 0.070	–0.066 ± 0.007	0.019 ± 0.070	–0.011 ± 0.113	–0.111 ± 0.070
179949	–0.017 ± 0.127	0.000 ± 0.070	–0.070 ± 0.028	0.020 ± 0.014	–0.120 ± 0.028	–0.260 ± 0.028
19994	0.018 ± 0.068	0.061 ± 0.070	0.061 ± 0.070	0.136 ± 0.021	–	–0.049 ± 0.070
208487	–0.064 ± 0.030	0.016 ± 0.070	–0.024 ± 0.070	0.016 ± 0.042	0.031 ± 0.106	–0.064 ± 0.028
212301	–0.094 ± 0.028	0.086 ± 0.070	–0.114 ± 0.057	–0.004 ± 0.071	–0.054 ± 0.057	–0.219 ± 0.021
216435	–	–0.044 ± 0.070	–0.024 ± 0.070	0.111 ± 0.021	–0.014 ± 0.014	0.006 ± 0.042
221287	–	0.037 ± 0.070	–0.178 ± 0.021	–0.078 ± 0.021	–0.113 ± 0.014	–0.173 ± 0.070
23079	–0.001 ± 0.045	0.103 ± 0.070	–0.047 ± 0.042	–0.022 ± 0.064	0.008 ± 0.021	–0.027 ± 0.028
39091	–	0.029 ± 0.070	–0.071 ± 0.028	0.039 ± 0.057	0.029 ± 0.042	–0.046 ± 0.035
7449	–0.039 ± 0.035	0.164 ± 0.070	–0.055 ± 0.042	–0.035 ± 0.057	–	–0.090 ± 0.007
75289	–0.168 ± 0.025	–0.165 ± 0.070	–0.155 ± 0.127	–0.050 ± 0.035	0.005 ± 0.042	–0.060 ± 0.007
82943	–0.069 ± 0.021	–0.036 ± 0.070	–0.056 ± 0.085	0.094 ± 0.070	–0.071 ± 0.120	–0.031 ± 0.021
93385	–0.045 ± 0.026	0.055 ± 0.070	–0.050 ± 0.064	0.040 ± 0.049	–0.025 ± 0.028	–0.015 ± 0.014
209458	0.011 ± 0.070	–0.099 ± 0.070	–0.084 ± 0.064	–0.044 ± 0.064	–	–0.089 ± 0.014
2039	–0.073 ± 0.106	–0.143 ± 0.070	–0.083 ± 0.042	0.107 ± 0.028	–0.123 ± 0.070	–0.003 ± 0.028
213240	–0.075 ± 0.025	0.061 ± 0.070	–0.122 ± 0.029	0.071 ± 0.042	0.041 ± 0.042	0.021 ± 0.028
23596	0.019 ± 0.076	–0.008 ± 0.070	–0.043 ± 0.035	0.162 ± 0.071	–0.018 ± 0.014	–0.008 ± 0.014
50554	0.033 ± 0.101	–0.094 ± 0.070	–0.129 ± 0.035	–0.064 ± 0.042	–0.034 ± 0.042	–0.084 ± 0.014
52265	–0.060 ± 0.047	0.053 ± 0.070	0.013 ± 0.057	0.078 ± 0.035	–	–0.057 ± 0.028
72659	0.020 ± 0.040	0.030 ± 0.070	–0.050 ± 0.085	0.060 ± 0.042	0.030 ± 0.070	0.010 ± 0.014
74156	–0.037 ± 0.025	0.006 ± 0.070	–0.054 ± 0.071	0.076 ± 0.057	0.026 ± 0.070	–0.034 ± 0.014
89744	–0.078 ± 0.014	–0.088 ± 0.070	–	0.052 ± 0.042	0.142 ± 0.070	–
9826	–0.003 ± 0.007	–0.078 ± 0.070	–	0.052 ± 0.042	0.102 ± 0.070	0.037 ± 0.148

Table A.2. Abundance ratios [X/Fe] of F-, G-type analogs with planets

HD	[Si/Fe]	[Ca/Fe]	[Sc/Fe]	[Ti/Fe]	[V/Fe]	[Cr/Fe]
10647	-0.031 ± 0.016	0.023 ± 0.024	-0.033 ± 0.031	-0.016 ± 0.031	-0.098 ± 0.049	-0.022 ± 0.040
108147	-0.010 ± 0.019	0.028 ± 0.021	-0.028 ± 0.010	-0.016 ± 0.033	-0.054 ± 0.041	-0.029 ± 0.025
117618	0.004 ± 0.018	0.024 ± 0.032	0.029 ± 0.030	-0.019 ± 0.016	-0.018 ± 0.006	-0.006 ± 0.017
121504	-0.016 ± 0.015	0.021 ± 0.024	0.000 ± 0.034	-0.014 ± 0.017	-0.050 ± 0.015	0.014 ± 0.007
134060	-0.006 ± 0.025	0.008 ± 0.013	0.039 ± 0.032	0.005 ± 0.017	-0.007 ± 0.041	-0.002 ± 0.017
169830	0.007 ± 0.016	0.014 ± 0.048	-0.004 ± 0.027	-0.014 ± 0.034	-0.064 ± 0.030	-0.021 ± 0.023
17051	-0.006 ± 0.029	0.017 ± 0.031	-0.004 ± 0.074	-0.003 ± 0.050	-0.021 ± 0.084	0.002 ± 0.019
179949	-0.013 ± 0.040	0.005 ± 0.033	-0.040 ± 0.010	-0.022 ± 0.037	-0.018 ± 0.058	-0.025 ± 0.026
19994	0.027 ± 0.032	-0.007 ± 0.029	0.076 ± 0.019	0.041 ± 0.044	-0.005 ± 0.075	-0.042 ± 0.056
208487	-0.004 ± 0.009	0.021 ± 0.010	0.004 ± 0.022	-0.004 ± 0.024	-0.062 ± 0.040	-0.018 ± 0.019
212301	-0.019 ± 0.034	0.014 ± 0.016	-0.014 ± 0.048	-0.016 ± 0.034	-0.006 ± 0.041	0.001 ± 0.021
216435	0.018 ± 0.015	0.019 ± 0.029	0.051 ± 0.025	-0.008 ± 0.035	0.012 ± 0.044	-0.018 ± 0.027
221287	-0.035 ± 0.014	0.044 ± 0.032	-0.028 ± 0.017	0.020 ± 0.034	-0.066 ± 0.088	-0.009 ± 0.043
23079	0.008 ± 0.007	0.051 ± 0.010	0.037 ± 0.036	0.029 ± 0.021	-0.064 ± 0.040	-0.002 ± 0.020
39091	0.001 ± 0.013	0.013 ± 0.017	0.019 ± 0.042	-0.018 ± 0.026	-0.038 ± 0.025	-0.002 ± 0.013
7449	0.001 ± 0.007	0.052 ± 0.018	-0.017 ± 0.026	0.020 ± 0.025	-0.054 ± 0.045	-0.000 ± 0.026
75289	-0.028 ± 0.028	0.045 ± 0.030	0.043 ± 0.054	0.010 ± 0.024	-0.018 ± 0.045	0.002 ± 0.014
82943	-0.006 ± 0.018	-0.036 ± 0.062	0.064 ± 0.037	-0.027 ± 0.026	-0.004 ± 0.023	0.000 ± 0.017
93385	0.008 ± 0.013	0.020 ± 0.010	0.028 ± 0.021	-0.006 ± 0.023	-0.035 ± 0.042	0.001 ± 0.019
209458	0.002 ± 0.056	0.041 ± 0.055	-	0.014 ± 0.090	-0.069 ± 0.029	0.024 ± 0.133
2039	-0.000 ± 0.017	0.014 ± 0.036	0.039 ± 0.047	-0.000 ± 0.029	0.047 ± 0.007	0.006 ± 0.012
213240	0.007 ± 0.012	0.008 ± 0.032	0.071 ± 0.055	0.008 ± 0.023	0.015 ± 0.025	-0.022 ± 0.016
23596	0.014 ± 0.039	-0.027 ± 0.045	0.105 ± 0.022	-0.025 ± 0.034	0.006 ± 0.023	-0.013 ± 0.039
50554	-0.009 ± 0.049	0.009 ± 0.034	0.049 ± 0.006	0.009 ± 0.049	0.008 ± 0.058	-0.025 ± 0.044
52265	0.015 ± 0.020	0.061 ± 0.033	0.028 ± 0.033	-0.027 ± 0.021	-0.031 ± 0.023	-0.015 ± 0.033
72659	0.021 ± 0.012	0.026 ± 0.014	0.050 ± 0.026	0.014 ± 0.015	-0.030 ± 0.038	-0.008 ± 0.008
74156	0.010 ± 0.010	0.030 ± 0.038	0.044 ± 0.010	0.000 ± 0.029	-0.017 ± 0.027	-0.034 ± 0.019
89744	0.015 ± 0.034	0.030 ± 0.034	0.035 ± 0.043	-0.021 ± 0.052	-0.036 ± 0.067	-0.038 ± 0.028
9826	0.032 ± 0.031	0.017 ± 0.014	0.080 ± 0.024	0.009 ± 0.058	0.010 ± 0.077	-0.043 ± 0.044

Table A.3. Abundance ratios [X/Fe] of F-, G-type analogs with planets

HD	[Mn/Fe]	[Co/Fe]	[Ni/Fe]	[Cu/Fe]	[Zn/Fe]	[Sr/Fe]
10647	-0.046 ± 0.083	-0.122 ± 0.037	-0.064 ± 0.024	-0.048 ± 0.070	-0.078 ± 0.028	0.092 ± 0.070
108147	-0.048 ± 0.033	-0.088 ± 0.024	-0.036 ± 0.030	-0.061 ± 0.070	-0.091 ± 0.042	0.069 ± 0.070
117618	-0.006 ± 0.026	-0.027 ± 0.009	0.003 ± 0.015	0.017 ± 0.070	0.007 ± 0.014	-0.043 ± 0.070
121504	-0.048 ± 0.021	-0.049 ± 0.005	-0.018 ± 0.016	-0.026 ± 0.070	-0.016 ± 0.057	0.024 ± 0.070
134060	-0.005 ± 0.028	-0.007 ± 0.006	0.008 ± 0.022	-0.007 ± 0.070	0.003 ± 0.085	-0.017 ± 0.070
169830	-0.052 ± 0.054	-0.035 ± 0.024	-0.011 ± 0.023	0.018 ± 0.070	-0.077 ± 0.021	-0.002 ± 0.070
17051	0.006 ± 0.046	-0.063 ± 0.027	-0.013 ± 0.027	-0.051 ± 0.070	-0.051 ± 0.028	0.039 ± 0.070
179949	0.028 ± 0.021	-0.066 ± 0.029	-0.025 ± 0.028	-0.050 ± 0.070	-0.110 ± 0.042	0.000 ± 0.070
19994	0.069 ± 0.017	0.006 ± 0.051	0.037 ± 0.028	0.121 ± 0.070	-0.059 ± 0.070	-0.019 ± 0.070
208487	-0.074 ± 0.067	-0.046 ± 0.029	-0.025 ± 0.019	-0.004 ± 0.070	-0.024 ± 0.057	-0.004 ± 0.070
212301	0.003 ± 0.094	-0.036 ± 0.056	-0.009 ± 0.030	0.006 ± 0.070	-0.064 ± 0.042	-0.034 ± 0.070
216435	0.042 ± 0.073	0.016 ± 0.015	0.028 ± 0.026	0.026 ± 0.070	0.011 ± 0.120	-0.104 ± 0.070
221287	-0.260 ± 0.103	-0.116 ± 0.034	-0.068 ± 0.032	-0.013 ± 0.070	-0.093 ± 0.070	0.107 ± 0.070
23079	-0.070 ± 0.070	-0.039 ± 0.024	-0.031 ± 0.014	-0.007 ± 0.070	-0.037 ± 0.014	-0.017 ± 0.070
39091	-0.009 ± 0.031	-0.025 ± 0.005	-0.003 ± 0.010	-0.001 ± 0.070	0.019 ± 0.042	-0.061 ± 0.070
7449	-0.063 ± 0.079	-0.085 ± 0.017	-0.044 ± 0.012	-0.035 ± 0.070	-0.055 ± 0.014	0.005 ± 0.070
75289	-0.060 ± 0.057	-0.039 ± 0.022	-0.015 ± 0.026	-0.065 ± 0.070	-0.145 ± 0.057	0.015 ± 0.070
82943	0.072 ± 0.019	0.010 ± 0.025	0.029 ± 0.019	0.004 ± 0.070	-0.006 ± 0.042	-0.086 ± 0.070
93385	-0.049 ± 0.045	-0.033 ± 0.017	-0.002 ± 0.012	-0.005 ± 0.070	0.000 ± 0.007	-0.035 ± 0.070
209458	-0.146 ± 0.062	-0.051 ± 0.133	-0.032 ± 0.110	–	-0.139 ± 0.070	-0.009 ± 0.070
2039	0.097 ± 0.070	0.033 ± 0.023	0.039 ± 0.038	-0.033 ± 0.070	-0.053 ± 0.070	–
213240	-0.014 ± 0.029	0.016 ± 0.012	0.013 ± 0.020	-0.009 ± 0.070	0.028 ± 0.040	-0.069 ± 0.070
23596	0.137 ± 0.031	0.019 ± 0.030	0.042 ± 0.029	–	0.062 ± 0.113	-0.108 ± 0.070
50554	-0.076 ± 0.102	-0.057 ± 0.025	-0.035 ± 0.037	–	-0.069 ± 0.134	0.216 ± 0.070
52265	-0.015 ± 0.067	-0.040 ± 0.031	0.006 ± 0.026	-0.017 ± 0.070	-0.007 ± 0.017	-0.007 ± 0.070
72659	-0.110 ± 0.071	0.005 ± 0.005	-0.007 ± 0.020	0.060 ± 0.070	-0.020 ± 0.070	–
74156	-0.059 ± 0.092	-0.004 ± 0.012	0.016 ± 0.028	0.046 ± 0.070	-0.034 ± 0.070	–
89744	0.082 ± 0.099	-0.074 ± 0.047	-0.038 ± 0.044	–	–	–
9826	–	-0.031 ± 0.032	-0.017 ± 0.039	–	-0.008 ± 0.070	–

Table A.4. Abundance ratios [X/Fe] of F-, G-type analogs with planets

HD	[Y/Fe]	[Zr/Fe]	[Ba/Fe]	[Ce/Fe]	[Nd/Fe]	[Eu/Fe]
10647	0.162 ± 0.026	0.172 ± 0.070	0.262 ± 0.042	0.135 ± 0.074	0.032 ± 0.070	0.062 ± 0.070
108147	0.124 ± 0.049	0.119 ± 0.070	0.124 ± 0.064	0.042 ± 0.006	-0.021 ± 0.070	0.169 ± 0.070
117618	0.047 ± 0.020	0.087 ± 0.070	0.057 ± 0.070	-0.070 ± 0.031	-0.003 ± 0.070	0.027 ± 0.070
121504	0.098 ± 0.035	0.114 ± 0.070	0.149 ± 0.021	0.038 ± 0.015	-0.026 ± 0.070	0.074 ± 0.070
134060	0.033 ± 0.040	0.053 ± 0.070	0.038 ± 0.021	0.003 ± 0.017	-0.137 ± 0.070	-0.027 ± 0.070
169830	0.068 ± 0.044	0.058 ± 0.070	0.033 ± 0.021	-0.055 ± 0.067	-0.082 ± 0.070	-0.052 ± 0.070
17051	0.092 ± 0.055	0.089 ± 0.070	0.128 ± 0.099	0.029 ± 0.026	-0.161 ± 0.070	0.039 ± 0.070
179949	0.050 ± 0.028	0.050 ± 0.070	0.020 ± 0.028	-0.027 ± 0.012	-0.120 ± 0.070	0.060 ± 0.070
19994	0.088 ± 0.090	0.141 ± 0.070	-0.124 ± 0.007	-0.022 ± 0.057	-0.079 ± 0.070	0.201 ± 0.070
208487	0.069 ± 0.050	0.086 ± 0.070	0.081 ± 0.021	0.049 ± 0.021	0.006 ± 0.070	0.026 ± 0.070
212301	0.062 ± 0.025	0.086 ± 0.070	-0.019 ± 0.021	-	-0.084 ± 0.070	0.025 ± 0.070
216435	0.050 ± 0.059	-0.024 ± 0.070	-0.009 ± 0.021	-0.030 ± 0.035	-0.124 ± 0.070	-0.084 ± 0.070
221287	0.174 ± 0.021	0.207 ± 0.070	0.297 ± 0.085	0.107 ± 0.123	0.067 ± 0.070	-0.013 ± 0.070
23079	0.089 ± 0.029	0.123 ± 0.070	0.113 ± 0.070	0.049 ± 0.051	0.013 ± 0.070	0.073 ± 0.070
39091	0.035 ± 0.031	-0.011 ± 0.070	0.019 ± 0.070	-0.011 ± 0.036	-0.111 ± 0.070	-0.051 ± 0.070
7449	0.101 ± 0.029	0.105 ± 0.070	0.185 ± 0.070	0.095 ± 0.052	0.025 ± 0.070	0.125 ± 0.070
75289	0.099 ± 0.042	0.095 ± 0.070	0.075 ± 0.070	0.009 ± 0.023	-0.045 ± 0.070	-0.055 ± 0.070
82943	-0.016 ± 0.040	0.014 ± 0.070	-0.051 ± 0.049	-0.039 ± 0.064	-0.116 ± 0.070	-0.056 ± 0.070
93385	0.042 ± 0.021	0.065 ± 0.070	0.080 ± 0.021	0.002 ± 0.035	-0.065 ± 0.070	0.025 ± 0.070
209458	-	-	0.211 ± 0.085	0.041 ± 0.072	-	0.081 ± 0.070
2039	0.001 ± 0.015	-0.043 ± 0.070	-0.108 ± 0.021	-	-	-0.073 ± 0.070
213240	0.005 ± 0.042	0.001 ± 0.070	-0.019 ± 0.028	-0.005 ± 0.006	-0.119 ± 0.070	0.011 ± 0.070
23596	0.042 ± 0.035	-0.028 ± 0.070	-0.108 ± 0.070	-0.118 ± 0.141	-0.208 ± 0.070	-0.128 ± 0.070
50554	0.163 ± 0.045	0.136 ± 0.070	0.136 ± 0.085	0.321 ± 0.092	0.026 ± 0.070	0.026 ± 0.070
52265	0.050 ± 0.047	0.063 ± 0.070	-0.012 ± 0.007	-0.071 ± 0.025	-0.107 ± 0.070	0.013 ± 0.070
72659	-0.030 ± 0.044	0.020 ± 0.070	-0.005 ± 0.007	-	-0.080 ± 0.070	-0.030 ± 0.070
74156	0.050 ± 0.058	-0.004 ± 0.070	-0.009 ± 0.021	-	-0.024 ± 0.070	0.056 ± 0.070
89744	-	0.142 ± 0.070	0.022 ± 0.070	-	-	0.182 ± 0.070
9826	-	0.232 ± 0.070	0.022 ± 0.028	-	-	0.102 ± 0.070

Table A.5. Abundance ratios [X/Fe] of F-, G-type analogs without known planets

HD	[C/Fe]	[O/Fe]	[S/Fe]	[Na/Fe]	[Mg/Fe]	[Al/Fe]
11226	0.060 ± 0.042	0.054 ± 0.070	0.083 ± 0.070	0.073 ± 0.042	–	–0.042 ± 0.021
119638	0.016 ± 0.044	0.116 ± 0.070	0.006 ± 0.057	0.021 ± 0.064	–0.029 ± 0.035	–0.054 ± 0.028
122862	0.050 ± 0.035	0.094 ± 0.070	–0.016 ± 0.042	0.044 ± 0.042	–0.001 ± 0.021	–0.021 ± 0.035
125881	–0.037 ± 0.070	–0.037 ± 0.070	–0.032 ± 0.049	–0.012 ± 0.035	–	–0.072 ± 0.021
1388	–0.068 ± 0.020	0.032 ± 0.070	–0.043 ± 0.078	0.002 ± 0.042	–0.068 ± 0.099	–0.033 ± 0.007
145666	–0.054 ± 0.071	–0.117 ± 0.070	–0.127 ± 0.070	–0.042 ± 0.035	–0.037 ± 0.014	–0.087 ± 0.028
157338	–0.011 ± 0.035	0.094 ± 0.070	–0.036 ± 0.028	0.009 ± 0.064	–0.016 ± 0.070	–0.056 ± 0.028
1581	0.004 ± 0.060	0.067 ± 0.070	–0.038 ± 0.007	0.022 ± 0.049	0.042 ± 0.035	–0.018 ± 0.035
168871	–	0.027 ± 0.070	0.007 ± 0.070	0.042 ± 0.035	0.052 ± 0.064	–0.003 ± 0.014
171990	0.034 ± 0.023	0.118 ± 0.070	0.068 ± 0.070	0.093 ± 0.049	0.038 ± 0.028	–0.017 ± 0.007
193193	0.002 ± 0.029	0.205 ± 0.070	–0.020 ± 0.064	0.055 ± 0.042	–0.010 ± 0.035	–0.005 ± 0.028
196800	–0.097 ± 0.060	0.063 ± 0.070	–0.007 ± 0.057	0.088 ± 0.035	–0.042 ± 0.064	–0.007 ± 0.070
199960	–0.021 ± 0.014	0.069 ± 0.070	–	0.059 ± 0.113	–0.056 ± 0.092	–0.021 ± 0.057
204385	0.005 ± 0.090	0.032 ± 0.070	–0.053 ± 0.035	0.052 ± 0.042	–0.003 ± 0.007	–0.018 ± 0.028
221356	–	0.115 ± 0.070	–0.175 ± 0.028	–0.070 ± 0.078	0.025 ± 0.071	–0.045 ± 0.028
31822	–0.061 ± 0.021	0.096 ± 0.070	–0.114 ± 0.070	–0.059 ± 0.049	–0.034 ± 0.070	–0.089 ± 0.035
36379	0.070 ± 0.026	0.110 ± 0.070	0.041 ± 0.070	0.055 ± 0.049	0.050 ± 0.042	–0.020 ± 0.014
3823	0.110 ± 0.085	0.227 ± 0.070	0.012 ± 0.064	0.032 ± 0.049	0.087 ± 0.071	–0.003 ± 0.042
38973	0.002 ± 0.025	–0.025 ± 0.070	–0.025 ± 0.057	0.025 ± 0.028	–0.030 ± 0.035	–0.030 ± 0.021
44120	–0.030 ± 0.038	–0.006 ± 0.070	–0.006 ± 0.070	0.069 ± 0.049	–0.036 ± 0.042	–0.016 ± 0.028
44447	0.060 ± 0.061	0.190 ± 0.070	–	0.030 ± 0.042	0.090 ± 0.085	–0.020 ± 0.014
6735	–0.029 ± 0.042	0.094 ± 0.070	–0.036 ± 0.127	–0.010 ± 0.035	–0.056 ± 0.042	–0.086 ± 0.028
68978A	–0.058 ± 0.017	–0.058 ± 0.070	–0.083 ± 0.134	0.002 ± 0.057	–0.003 ± 0.007	–0.048 ± 0.028
69655	0.026 ± 0.021	0.143 ± 0.070	–0.022 ± 0.021	0.053 ± 0.042	0.017 ± 0.021	–0.022 ± 0.021
70889	–0.127 ± 0.025	–0.044 ± 0.070	–0.079 ± 0.120	–0.044 ± 0.057	–0.064 ± 0.014	–0.104 ± 0.070
71479	–0.044 ± 0.035	0.133 ± 0.070	–0.057 ± 0.071	0.058 ± 0.106	–0.027 ± 0.057	–0.012 ± 0.007
73121	–0.053 ± 0.020	0.077 ± 0.070	–0.103 ± 0.070	0.037 ± 0.071	0.007 ± 0.070	0.007 ± 0.014
73524	–0.160 ± 0.007	–0.055 ± 0.070	–0.125 ± 0.071	–0.075 ± 0.042	–0.065 ± 0.085	–0.030 ± 0.035
88742	–0.003 ± 0.032	0.041 ± 0.070	–0.029 ± 0.071	–0.029 ± 0.057	–0.029 ± 0.014	–0.084 ± 0.021
95456	–0.068 ± 0.021	–0.012 ± 0.070	–0.012 ± 0.099	0.028 ± 0.057	–0.052 ± 0.014	–0.082 ± 0.028
9782	–0.002 ± 0.045	0.015 ± 0.070	–0.015 ± 0.099	0.025 ± 0.057	–0.055 ± 0.042	–0.060 ± 0.035
33636	–0.106 ± 0.015	0.061 ± 0.070	–0.114 ± 0.021	–0.039 ± 0.057	0.161 ± 0.070	–0.054 ± 0.021

Table A.6. Abundance ratios [X/Fe] of F-, G-type analogs without known planets

HD	[Si/Fe]	[Ca/Fe]	[Sc/Fe]	[Ti/Fe]	[V/Fe]	[Cr/Fe]
11226	0.012 ± 0.011	0.003 ± 0.017	0.032 ± 0.051	-0.021 ± 0.024	-0.030 ± 0.043	-0.007 ± 0.017
119638	0.027 ± 0.009	0.056 ± 0.028	0.023 ± 0.026	0.015 ± 0.023	-0.042 ± 0.026	-0.004 ± 0.022
122862	0.027 ± 0.009	0.041 ± 0.031	0.071 ± 0.026	0.015 ± 0.013	-0.035 ± 0.051	-0.003 ± 0.024
125881	-0.011 ± 0.022	0.023 ± 0.014	-0.019 ± 0.037	-0.019 ± 0.017	-0.043 ± 0.018	0.005 ± 0.010
1388	0.002 ± 0.014	0.036 ± 0.014	0.042 ± 0.043	0.007 ± 0.017	-0.072 ± 0.024	-0.007 ± 0.020
145666	-0.031 ± 0.010	0.019 ± 0.013	-0.052 ± 0.017	-0.014 ± 0.016	-0.077 ± 0.030	0.008 ± 0.012
157338	-0.002 ± 0.009	0.024 ± 0.023	0.009 ± 0.024	-0.008 ± 0.013	-0.056 ± 0.045	-0.006 ± 0.022
1581	0.030 ± 0.007	0.056 ± 0.018	0.040 ± 0.027	0.045 ± 0.027	-0.033 ± 0.055	-0.014 ± 0.020
168871	0.017 ± 0.017	0.056 ± 0.034	0.057 ± 0.043	0.007 ± 0.016	-0.030 ± 0.040	-0.007 ± 0.023
171990	0.022 ± 0.012	0.041 ± 0.047	0.060 ± 0.041	-0.005 ± 0.017	-0.028 ± 0.029	-0.012 ± 0.017
193193	0.010 ± 0.009	0.015 ± 0.018	0.063 ± 0.038	0.005 ± 0.016	-0.013 ± 0.025	-0.002 ± 0.019
196800	0.003 ± 0.017	-0.017 ± 0.014	0.045 ± 0.038	-0.025 ± 0.030	-0.002 ± 0.044	-0.010 ± 0.034
199960	0.015 ± 0.019	-0.021 ± 0.063	0.057 ± 0.035	-0.017 ± 0.035	0.007 ± 0.032	-0.008 ± 0.020
204385	0.011 ± 0.017	0.012 ± 0.022	0.042 ± 0.027	-0.013 ± 0.026	-0.058 ± 0.033	0.005 ± 0.018
221356	0.012 ± 0.012	0.069 ± 0.049	0.075 ± 0.016	0.088 ± 0.036	-0.069 ± 0.039	-0.025 ± 0.031
31822	-0.001 ± 0.014	0.054 ± 0.025	-0.022 ± 0.022	0.014 ± 0.040	-0.104 ± 0.028	0.005 ± 0.025
36379	0.044 ± 0.011	0.062 ± 0.029	0.070 ± 0.033	0.021 ± 0.024	-0.020 ± 0.053	0.006 ± 0.023
3823	0.061 ± 0.019	0.080 ± 0.021	0.072 ± 0.033	0.058 ± 0.029	-0.035 ± 0.050	-0.008 ± 0.020
38973	0.006 ± 0.012	0.021 ± 0.017	0.003 ± 0.030	-0.023 ± 0.019	-0.033 ± 0.035	0.004 ± 0.018
44120	0.004 ± 0.019	0.035 ± 0.049	0.031 ± 0.022	-0.020 ± 0.024	-0.008 ± 0.025	-0.020 ± 0.020
44447	0.039 ± 0.009	0.051 ± 0.016	0.058 ± 0.040	0.025 ± 0.019	-0.033 ± 0.055	-0.007 ± 0.020
6735	0.011 ± 0.012	0.057 ± 0.021	-0.002 ± 0.033	0.009 ± 0.034	-0.075 ± 0.047	-0.010 ± 0.019
68978A	0.001 ± 0.011	0.030 ± 0.023	-0.003 ± 0.017	-0.006 ± 0.013	-0.037 ± 0.039	0.011 ± 0.013
69655	0.019 ± 0.009	0.038 ± 0.024	0.025 ± 0.022	0.006 ± 0.019	-0.062 ± 0.043	-0.004 ± 0.013
70889	-0.028 ± 0.008	0.021 ± 0.024	-0.039 ± 0.045	-0.026 ± 0.027	-0.064 ± 0.023	0.008 ± 0.014
71479	-0.001 ± 0.019	-0.015 ± 0.026	0.083 ± 0.041	-0.003 ± 0.017	0.029 ± 0.022	-0.000 ± 0.019
73121	0.016 ± 0.015	0.015 ± 0.017	0.060 ± 0.036	-0.000 ± 0.024	-0.006 ± 0.043	-0.008 ± 0.026
73524	-0.008 ± 0.014	0.044 ± 0.030	0.005 ± 0.022	0.010 ± 0.020	-0.030 ± 0.024	0.006 ± 0.016
88742	-0.014 ± 0.013	0.019 ± 0.026	-0.044 ± 0.034	-0.029 ± 0.019	-0.043 ± 0.023	0.013 ± 0.016
95456	0.000 ± 0.014	0.028 ± 0.047	-0.009 ± 0.015	-0.010 ± 0.034	-0.060 ± 0.037	-0.003 ± 0.024
9782	-0.014 ± 0.020	-0.010 ± 0.048	-0.018 ± 0.021	-0.045 ± 0.018	-0.042 ± 0.044	-0.013 ± 0.019
33636	0.004 ± 0.006	0.051 ± 0.015	0.015 ± 0.042	0.041 ± 0.022	-0.031 ± 0.038	0.008 ± 0.027

Table A.7. Abundance ratios [X/Fe] of F-, G-type analogs without known planets

HD	[Mn/Fe]	[Co/Fe]	[Ni/Fe]	[Cu/Fe]	[Zn/Fe]	[Sr/Fe]
11226	-0.057 ± 0.058	-0.022 ± 0.016	0.004 ± 0.018	0.003 ± 0.070	0.008 ± 0.035	-0.036 ± 0.070
119638	-0.097 ± 0.036	-0.033 ± 0.025	-0.025 ± 0.014	0.006 ± 0.070	-0.014 ± 0.042	-0.035 ± 0.070
122862	-0.039 ± 0.070	-0.028 ± 0.010	-0.010 ± 0.013	0.044 ± 0.070	0.019 ± 0.007	-0.096 ± 0.070
125881	-0.057 ± 0.038	-0.069 ± 0.012	-0.024 ± 0.015	-0.027 ± 0.070	-0.017 ± 0.028	0.033 ± 0.070
1388	-0.082 ± 0.046	-0.038 ± 0.012	-0.021 ± 0.014	-0.008 ± 0.070	-0.043 ± 0.021	-0.008 ± 0.070
145666	-0.089 ± 0.045	-0.089 ± 0.007	-0.048 ± 0.015	-0.037 ± 0.070	-0.037 ± 0.042	0.053 ± 0.070
157338	-0.031 ± 0.071	-0.054 ± 0.024	-0.024 ± 0.012	-0.006 ± 0.070	0.019 ± 0.035	-0.026 ± 0.070
1581	-0.118 ± 0.039	-0.007 ± 0.022	-0.024 ± 0.014	-0.003 ± 0.070	0.007 ± 0.014	-0.043 ± 0.070
168871	-0.081 ± 0.106	-0.035 ± 0.016	-0.012 ± 0.013	0.027 ± 0.070	0.037 ± 0.028	-0.053 ± 0.070
171990	-0.056 ± 0.065	0.016 ± 0.028	0.013 ± 0.021	0.048 ± 0.070	0.033 ± 0.021	-0.062 ± 0.070
193193	-0.050 ± 0.026	-0.016 ± 0.021	-0.011 ± 0.015	0.005 ± 0.070	0.015 ± 0.014	-0.065 ± 0.070
196800	0.015 ± 0.015	0.015 ± 0.019	0.028 ± 0.017	0.013 ± 0.070	0.013 ± 0.057	-0.057 ± 0.070
199960	0.087 ± 0.025	0.059 ± 0.013	0.056 ± 0.028	0.059 ± 0.070	0.069 ± 0.113	-0.091 ± 0.070
204385	-0.024 ± 0.048	0.009 ± 0.014	0.001 ± 0.020	0.032 ± 0.070	0.036 ± 0.092	-0.128 ± 0.070
221356	-0.155 ± 0.073	-0.035 ± 0.035	-0.020 ± 0.037	0.075 ± 0.070	-0.105 ± 0.057	0.005 ± 0.070
31822	-0.162 ± 0.054	-0.086 ± 0.033	-0.057 ± 0.015	-0.004 ± 0.070	-0.099 ± 0.049	-0.004 ± 0.070
36379	-0.069 ± 0.078	-0.020 ± 0.023	-0.015 ± 0.015	0.030 ± 0.070	0.000 ± 0.070	-0.100 ± 0.070
3823	-0.153 ± 0.027	-0.002 ± 0.016	-0.013 ± 0.015	0.067 ± 0.070	-0.028 ± 0.078	-0.093 ± 0.070
38973	-0.045 ± 0.037	-0.031 ± 0.013	-0.001 ± 0.013	-0.005 ± 0.070	0.010 ± 0.035	-0.055 ± 0.070
44120	-0.016 ± 0.055	-0.016 ± 0.008	0.013 ± 0.015	0.014 ± 0.070	-0.001 ± 0.078	-0.076 ± 0.070
44447	-0.120 ± 0.039	-0.029 ± 0.033	-0.025 ± 0.015	0.020 ± 0.070	0.015 ± 0.021	-0.130 ± 0.070
6735	-0.144 ± 0.084	-0.061 ± 0.032	-0.042 ± 0.016	-0.025 ± 0.070	-0.050 ± 0.007	-0.005 ± 0.070
68978A	-0.082 ± 0.044	-0.028 ± 0.019	-0.017 ± 0.014	-0.028 ± 0.070	-0.143 ± 0.007	-0.218 ± 0.070
69655	-0.095 ± 0.039	-0.011 ± 0.015	-0.016 ± 0.018	0.013 ± 0.070	0.032 ± 0.085	-0.057 ± 0.070
70889	-0.024 ± 0.024	-0.082 ± 0.016	-0.033 ± 0.009	-0.064 ± 0.070	-0.074 ± 0.028	0.046 ± 0.070
71479	0.037 ± 0.043	0.033 ± 0.018	0.041 ± 0.015	0.023 ± 0.070	0.003 ± 0.042	-0.037 ± 0.070
73121	-0.033 ± 0.033	-0.021 ± 0.013	0.001 ± 0.017	0.007 ± 0.070	0.002 ± 0.035	-0.033 ± 0.070
73524	-0.060 ± 0.024	-0.022 ± 0.013	-0.012 ± 0.015	-0.045 ± 0.070	-0.095 ± 0.042	0.055 ± 0.070
88742	-0.057 ± 0.022	-0.071 ± 0.022	-0.034 ± 0.014	-0.069 ± 0.070	-0.044 ± 0.007	0.031 ± 0.070
95456	-0.029 ± 0.039	-0.035 ± 0.022	-0.010 ± 0.018	-0.002 ± 0.070	-0.047 ± 0.007	-0.012 ± 0.070
9782	-0.020 ± 0.029	-0.038 ± 0.020	-0.005 ± 0.019	-0.025 ± 0.070	-0.050 ± 0.035	-0.025 ± 0.070
33636	–	-0.062 ± 0.016	-0.047 ± 0.017	-0.079 ± 0.070	-0.039 ± 0.070	–

Table A.8. Abundance ratios [X/Fe] of F-, G-type analogs without known planets

HD	[Y/Fe]	[Zr/Fe]	[Ba/Fe]	[Ce/Fe]	[Nd/Fe]	[Eu/Fe]
11226	0.030 ± 0.029	0.044 ± 0.070	0.048 ± 0.106	-0.047 ± 0.030	-0.117 ± 0.070	0.003 ± 0.070
119638	0.056 ± 0.035	0.096 ± 0.070	0.126 ± 0.042	-0.001 ± 0.076	-0.054 ± 0.070	0.046 ± 0.070
122862	0.000 ± 0.046	0.034 ± 0.070	0.024 ± 0.028	-0.046 ± 0.060	-0.056 ± 0.070	0.074 ± 0.070
125881	0.103 ± 0.010	0.133 ± 0.070	0.148 ± 0.049	0.019 ± 0.038	-0.027 ± 0.070	0.063 ± 0.070
1388	0.048 ± 0.021	0.072 ± 0.070	0.067 ± 0.007	0.028 ± 0.025	-0.078 ± 0.070	0.042 ± 0.070
145666	0.119 ± 0.012	0.133 ± 0.070	0.198 ± 0.007	0.096 ± 0.029	0.003 ± 0.070	0.033 ± 0.070
157338	0.057 ± 0.015	0.074 ± 0.070	0.129 ± 0.106	-0.003 ± 0.025	-0.086 ± 0.070	0.014 ± 0.070
1581	0.040 ± 0.023	0.107 ± 0.070	0.097 ± 0.028	0.040 ± 0.050	0.007 ± 0.070	0.097 ± 0.070
168871	0.024 ± 0.029	0.057 ± 0.070	0.052 ± 0.021	-0.006 ± 0.021	-0.083 ± 0.070	0.077 ± 0.070
171990	0.044 ± 0.038	0.048 ± 0.070	0.043 ± 0.021	-0.032 ± 0.061	-0.102 ± 0.070	0.028 ± 0.070
193193	0.015 ± 0.026	-0.015 ± 0.070	0.060 ± 0.021	-0.018 ± 0.029	-0.095 ± 0.070	-0.015 ± 0.070
196800	0.013 ± 0.026	-0.067 ± 0.070	-0.037 ± 0.014	-0.034 ± 0.092	-0.127 ± 0.070	-0.167 ± 0.070
199960	-0.008 ± 0.075	0.009 ± 0.070	-0.076 ± 0.035	-	-0.161 ± 0.070	0.059 ± 0.070
204385	0.045 ± 0.023	-0.048 ± 0.070	0.061 ± 0.028	-0.035 ± 0.050	-0.088 ± 0.070	-0.008 ± 0.070
221356	0.052 ± 0.061	0.075 ± 0.070	0.215 ± 0.014	-	0.065 ± 0.070	0.145 ± 0.070
31822	0.092 ± 0.012	0.096 ± 0.070	0.271 ± 0.035	0.122 ± 0.086	0.066 ± 0.070	-0.094 ± 0.070
36379	-0.020 ± 0.044	0.020 ± 0.070	0.030 ± 0.042	-0.050 ± 0.026	-0.089 ± 0.070	0.041 ± 0.070
3823	-0.043 ± 0.053	0.017 ± 0.070	-0.028 ± 0.021	-0.033 ± 0.050	-0.083 ± 0.070	0.077 ± 0.070
38973	0.052 ± 0.021	0.035 ± 0.070	0.030 ± 0.035	-0.042 ± 0.035	-0.075 ± 0.070	0.025 ± 0.070
44120	0.014 ± 0.026	0.014 ± 0.070	0.019 ± 0.007	-0.046 ± 0.020	-0.116 ± 0.070	0.034 ± 0.070
44447	-0.047 ± 0.049	-0.010 ± 0.070	-0.010 ± 0.014	-0.050 ± 0.062	-0.100 ± 0.070	0.030 ± 0.070
6735	0.101 ± 0.029	0.134 ± 0.070	0.194 ± 0.028	0.041 ± 0.137	-0.036 ± 0.070	-0.005 ± 0.070
68978A	0.079 ± 0.029	0.042 ± 0.070	0.122 ± 0.028	0.032 ± 0.017	-0.068 ± 0.070	-0.098 ± 0.070
69655	0.002 ± 0.026	0.023 ± 0.070	0.058 ± 0.007	-0.007 ± 0.017	-0.047 ± 0.070	0.032 ± 0.070
70889	0.113 ± 0.012	0.116 ± 0.070	0.176 ± 0.028	0.053 ± 0.015	-0.084 ± 0.070	-0.054 ± 0.070
71479	0.010 ± 0.051	-0.017 ± 0.070	-0.047 ± 0.028	-0.044 ± 0.049	-0.157 ± 0.070	-0.027 ± 0.070
73121	0.067 ± 0.044	0.047 ± 0.070	0.107 ± 0.042	0.020 ± 0.046	-0.083 ± 0.070	0.067 ± 0.070
73524	0.085 ± 0.040	0.105 ± 0.070	0.095 ± 0.014	0.042 ± 0.025	-0.055 ± 0.070	0.045 ± 0.070
88742	0.097 ± 0.021	0.131 ± 0.070	0.151 ± 0.014	0.051 ± 0.030	-0.049 ± 0.070	-0.039 ± 0.070
95456	0.078 ± 0.044	0.058 ± 0.070	0.028 ± 0.070	-0.025 ± 0.032	-0.052 ± 0.070	-0.052 ± 0.070
9782	0.058 ± 0.015	0.045 ± 0.070	0.030 ± 0.021	-0.065 ± 0.078	-0.145 ± 0.070	-0.045 ± 0.070
33636	0.101 ± 0.017	0.141 ± 0.070	0.191 ± 0.014	-	0.071 ± 0.070	0.051 ± 0.070